

**Exponential
eigenmodes of the
carbon-climate
system**

M. R. Raupach

The exponential eigenmodes of the carbon-climate system

M. R. Raupach¹

¹CSIRO Marine and Atmospheric Research, Canberra, ACT 2601, Australia

Received: 30 July 2012 – Accepted: 3 September 2012 – Published: 19 September 2012

Correspondence to: M. R. Raupach (michael.raupach@csiro.au)

Published by Copernicus Publications on behalf of the European Geosciences Union.

Title Page

Abstract

Introduction

Conclusions

References

Tables

Figures

⏪

⏩

◀

▶

Back

Close

Full Screen / Esc

Printer-friendly Version

Interactive Discussion

Abstract

Several basic ratios describing the carbon-climate system are observed to adopt relatively steady values. Examples include the CO₂ airborne fraction (the fraction of the total anthropogenic CO₂ emission flux that accumulates in the atmosphere) and the ratio T/Q_E of warming (T) to cumulative total CO₂ emissions (Q_E). This paper explores the reason for such near-constancy in the past, and its likely limitations in future.

The contemporary carbon-climate system is often approximated as a first-order linear system, for example in response-function descriptions. All such linear systems have exponential eigenfunctions in time (an eigenfunction being one that, if applied to the system as a forcing, produces a response of the same shape). This implies that, if the carbon-climate system is idealised as a linear system (Lin) forced by exponentially growing CO₂ emissions (Exp), then all ratios among fluxes and perturbation state variables are constant. Important cases are the CO₂ airborne fraction (AF), the cumulative airborne fraction (CAF), other CO₂ partition fractions and cumulative partition fractions into land and ocean stores, the CO₂ sink uptake rate (k_S , the combined land and ocean CO₂ sink flux per unit excess atmospheric CO₂), and the ratio T/Q_E . Further, the AF and the CAF are equal. The Lin and Exp idealisations apply approximately (but not exactly) to the carbon-climate system in the period from the start of industrialisation (nominally 1750) to the present, consistent with the observed near-constancy of the AF, CAF and T/Q_E in this period.

A nonlinear carbon-climate model is used to explore how the likely future breakdown of both the Lin and Exp idealisations will cause the AF, CAF and k_S to depart significantly from constancy, in ways that depend on CO₂ emissions scenarios. However, T/Q_E remains approximately constant in typical scenarios, because of compensating interactions between emissions trajectories, carbon-cycle dynamics and non-CO₂ gases. This theory assists in establishing both the basis and limits of the widely-assumed proportionality between T and Q_E , at about 2 K per trillion tonnes of carbon.

Exponential eigenmodes of the carbon-climate system

M. R. Raupach

Title Page

Abstract

Introduction

Conclusions

References

Tables

Figures



Back

Close

Full Screen / Esc

Printer-friendly Version

Interactive Discussion



1 Introduction

The global carbon-climate system has a number of stable properties, despite massive anthropogenic perturbation since the onset of industrialisation in the 18th century. The CO₂ airborne fraction (the fraction of the total anthropogenic CO₂ emission flux that accumulates in the atmosphere) has stayed close to a mean of about 0.44 for the last 50 yr, despite significant interannual variability and a small observed trend (Le Quéré et al., 2009). The ratio T/Q_E of warming (T) to cumulative total CO₂ emissions (Q_E) is also conservative, not only in the past but in future projections (Allen et al., 2009; Meinshausen et al., 2009; Matthews et al., 2009; Raupach et al., 2011), at around 2 K per trillion tonnes of carbon.

This paper investigates the conditions under which ratios like the airborne fraction and T/Q_E are conservative, and the limits of such conservative behaviour. The approach is to identify some general analytic properties of linearised models of the carbon-climate system, and then to test the limits of this idealisation. This is done in three steps, tackled respectively in Sects. 2, 3 and 4. First, it is shown in Sect. 2 that a wide class of first-order linear systems has exponential eigenfunctions (functions that, when applied to the system as a forcing, produce a response of the same shape), and that for this class of systems, all ratios among fluxes and perturbation state variables are constant. Next, in Sect. 3, this basic theorem is applied to the carbon-climate system under a “LinExp” idealisation, in which the system is linear or linearised (Lin) and is forced with exponentially growing anthropogenic CO₂ emissions (Exp). In this idealisation, constant ratios include the CO₂ airborne fraction, its cumulative counterpart, other CO₂ partition fractions, the CO₂ sink uptake rate, and the ratio T/Q_E . These predictions are tested directly against observations. Finally, in Sect. 4, the predictions of the LinExp idealisation are compared with predictions from a nonlinear model of the carbon-climate system, to investigate the applicability of the LinExp idealisation to future projections. Mathematical and modelling details are given in Appendices A and B, respectively.

Exponential eigenmodes of the carbon-climate system

M. R. Raupach

Title Page

Abstract

Introduction

Conclusions

References

Tables

Figures



Back

Close

Full Screen / Esc

Printer-friendly Version

Interactive Discussion



Exponential eigenmodes of the carbon-climate system

M. R. Raupach

Title Page

Abstract

Introduction

Conclusions

References

Tables

Figures

⏪

⏩

◀

▶

Back

Close

Full Screen / Esc

Printer-friendly Version

Interactive Discussion

The restricted LinExp world is not as great a distortion of current reality as might at first appear. Assumption Exp is historically approximately true for total CO₂ emissions from fossil fuel combustion and net deforestation from 1750 to 2010. CO₂ is the dominant net anthropogenic radiative forcing, because of the near-cancellation in the past of anthropogenic forcing from non-CO₂ gases and the forcing from non-gaseous influences, mainly aerosols (IPCC, 2007). Assumption Lin is widely used in the form of response-function models describing the response of the global carbon cycle to forcing from CO₂ emissions (for example, Joos et al., 1996; Trudinger et al., 2002; Enting, 2007; Li et al., 2009), and the response of the global climate system to specified radiative forcing (for example, Huntingford and Cox, 2000; Hansen et al., 2008; Li and Jarvis, 2009). Linearity of carbon-cycle and climate subsystems is also assumed in response-function models of the coupled carbon-climate system that incorporate weak nonlinearities in coupling between linear model components, for example through the dependence of CO₂ radiative forcing and ocean-air and land-air carbon exchanges on CO₂ concentration (Hasselmann et al., 1997; Petschel-Held et al., 1999; Hooss et al., 2001; Joos et al., 2001, 2012; Raper et al., 2001). Fully linear versions of such models can always be developed within a limited subspace around any given state of the Earth System, because a weakly nonlinear carbon-climate model can be linearised about that state. For these reasons, the LinExp idealisation turns out to be a useful approximate description of many aspects of the carbon-climate system from the 18th to the early 21st century. However, both the Lin and Exp assumptions will almost certainly break down in future, with consequences to be investigated in Sect. 4.

The mathematical analysis in this paper was presaged many years ago by Bacastow and Keeling (1979), who showed that the CO₂ airborne fraction and related flux partition ratios are constant in the LinExp idealisation. Here, this is extended to all ratios between fluxes and state variables in the coupled carbon-climate system, and the limits of the idealisation are explored.

2 Theory

2.1 General and linearised carbon-climate models

A model for the carbon-climate system can be regarded as a set of nonlinear equations

$$5 \quad dx/dt = f(t) + \Phi(x) \quad (1)$$

where $x(t)$ is a carbon-climate state vector of matter and energy stores (here taken to be perturbations about a preindustrial equilibrium state $x = 0$), $f(t)$ a vector of anthropogenic forcing fluxes, $\Phi(x)$ a vector of system response fluxes, and t time. The forcing flux vector $f(t)$ is externally prescribed. The response flux vector $\Phi(x)$, the net fluxes
10 into different stores (x) arising from the response of the system to forcing, is specified by nonlinear “phenomenological equations” embodying model parameterisations.

Equation (1) is a general representation of a carbon-climate model of any sophistication. The dimension of the state vector $x(t)$ may be of order 10 for a simple, globally aggregated model, or 10^7 for a sophisticated, spatially resolved model.

15 The response flux vector $\Phi(x)$ can be linearised as $-\mathbf{K}x$, where $-\mathbf{K}$ is the system response matrix (see Appendix A1). Then, Eq. (1) becomes a linear system of first-order ordinary differential equations:

$$dx/dt = f(t) - \mathbf{K}x \quad \text{with} \quad x(0) = 0. \quad (2)$$

The solution of this linear system for state variables $x(t)$ is

$$20 \quad x(t) = \int_0^t \mathbf{G}(t - \tau) f(\tau) d\tau \quad (3)$$

where $\mathbf{G}(t)$ is the matrix pulse response function (PRF) or Green’s function for the system (see references in the Introduction for carbon-climate applications). The element

Exponential eigenmodes of the carbon-climate system

M. R. Raupach

Title Page

Abstract

Introduction

Conclusions

References

Tables

Figures

⏪

⏩

◀

▶

Back

Close

Full Screen / Esc

Printer-friendly Version

Interactive Discussion



$G_{ij}(t)$ of $\mathbf{G}(t)$ is the fraction of a pulse input at time $t = 0$ into store j that appears at time t in store i . Formally, the PRF is given by $\mathbf{G}(t) = \mathbf{exp}(-\mathbf{K}t)$, where \mathbf{exp} denotes the matrix exponential (Glendinning, 1994); a more practical expression for $\mathbf{G}(t)$ is given below.

2.2 Normal modes

In Eq. (2), the system response matrix \mathbf{K} has off-diagonal terms representing coupling or feedback between different components of \mathbf{x} . A standard technique for treating coupled linear problems of this sort is the method of normal modes (Gershenfeld, 1999, p. 12; Enting, 2007). The principle (see Appendix A2 for detail) is to transform the state space into a reference frame in which \mathbf{K} becomes a diagonal matrix $\mathbf{\Lambda}$ and the state variables $\mathbf{x}(t)$ become new variables $\mathbf{y}(t)$, the “normal modes”. In the new reference frame, Eq. (2) becomes:

$$d\mathbf{y}/dt = \mathbf{U}^{-1}\mathbf{f}(t) - \mathbf{\Lambda}\mathbf{y} \quad \text{with} \quad \mathbf{y}(0) = 0 \quad (4)$$

where \mathbf{U} is the matrix of column eigenvectors of \mathbf{K} , and $\mathbf{\Lambda}$ is the diagonal matrix of its eigenvalues, $\lambda^{(m)}$ (see Appendix A2). Because $\mathbf{\Lambda}$ is diagonal, this is a set of independent scalar equations that can be solved one by one. When the solution $\mathbf{y}(t)$ of Eq. (4) is transformed back to the original reference frame to yield $\mathbf{x}(t)$, the result is Eq. (3), with the elements $G_{ij}(t)$ of the PRF explicitly identified as weighted sums of decaying exponential terms:

$$G_{ij}(t) = \sum_m a_{ij}^{(m)} \mathbf{exp}(-\lambda^{(m)}t). \quad (5)$$

The decay rates are the eigenvalues $\lambda^{(m)}$ of \mathbf{K} , and the weights $a_{ij}^{(m)}$ are specified by the eigenvectors of \mathbf{K} (see Eqs. A15 and A16).

It is assumed henceforth, subject to checking later, that the exponentials in $G_{ij}(t)$ decay in time. This occurs when all eigenvalues $\lambda^{(m)}$ of \mathbf{K} have positive real parts, so that the system defined by Eq. (2) is dynamically stable.

Exponential eigenmodes of the carbon-climate system

M. R. Raupach

Title Page

Abstract

Introduction

Conclusions

References

Tables

Figures

⏪

⏩

◀

▶

Back

Close

Full Screen / Esc

Printer-friendly Version

Interactive Discussion



2.3 Eigenfunctions

A linear system can be construed as a differential linear operator L acting on an input $x(t)$ to produce an output $L(x(t))$. For the linear system of Eq. (2), the linear operator is

$$L(x(t)) = \left(\frac{d}{dt} + \mathbf{K} \right) x(t) \quad (6)$$

so that Eq. (2) becomes $L(x(t)) = f(t)$.

An important attribute of any linear operator L is its set of eigenfunctions $\mathbf{v}(t)$, the functions for which the output is proportional to the input, so that $L(\mathbf{v}(t)) = \alpha \mathbf{v}(t)$. The proportionality coefficient α is the eigenvalue corresponding to the eigenfunction $\mathbf{v}(t)$. An eigenmode is described by both α and $\mathbf{v}(t)$. If a linear system is forced with an eigenfunction, so that $f(t)$ is proportional to $\mathbf{v}(t)$, then its response is the same eigenfunction.

For a first-order linear system, the eigenfunctions are exponentials in time (see Appendix A3 for the demonstration of this key fact). Therefore, an exponential forcing produces an exponential response with the same growth rate.

2.4 Ratios among fluxes and state variables

The exponential nature of the eigenfunctions for a first-order linear system implies the following for LinExp systems: (a) all state variables grow at forcing rates, not response rates; (b) all ratios among state variables approach constant values; (c) all partition fractions (ratios of growth rates of state variables to the forcing flux) approach constant values; and (d) all ratios become independent of initial conditions faster than forcing rates. Sketch proofs are given in Appendix A4, using theory similar to Bacastow and Keeling (1979, their Appendix B).

These properties can be illustrated for one-dimensional systems obeying the scalar counterpart of Eq. (2), $x'(t) = f(t) - kx$ (where the prime denotes a time derivative,

Exponential eigenmodes of the carbon-climate system

M. R. Raupach

Title Page

Abstract

Introduction

Conclusions

References

Tables

Figures

⏪

⏩

◀

▶

Back

Close

Full Screen / Esc

Printer-friendly Version

Interactive Discussion



Exponential eigenmodes of the carbon-climate system

M. R. Raupach

Title Page

Abstract

Introduction

Conclusions

References

Tables

Figures

◀

▶

◀

▶

Back

Close

Full Screen / Esc

Printer-friendly Version

Interactive Discussion

$x'(t) = dx/dt$). The scalar partition fraction is the ratio $x'(t)/f(t)$, the fraction of the forcing that appears instantaneously as increase in $x(t)$. The cumulative partition fraction is $x(t)/Q(-\infty, t)$, the ratio of the response $x(t)$ to the cumulative forcing $Q(-\infty, t)$, where the cumulative forcing is the integral of $f(t)$ from time $-\infty$ to t . For a LinExp system, the partition fraction (x'/f) and the cumulative partition fraction (x/Q) both approach the same constant value (Appendix A4, Eq. A27):

$$\frac{x'(t)}{f(t)} = \frac{x(t)}{Q(t)} = \frac{r}{r+k} + \text{transient.} \quad (7)$$

The transient term decays at the rate $r+k$. Since r and k are both positive for the systems under consideration, this is larger than both the forcing rate (r) and the response rate (k).

In the multi-dimensional case, the partition fractions are the fractions of the forcing flux entering the stores $x_i(t)$, and the cumulative partition fractions are the ratios of the stores themselves to cumulative forcing. For a LinExp system, these fractions approach constant values with decaying transient terms. When the system is forced exponentially with a growth rate r_1 in just the first component of the state vector \mathbf{x} , the partition fraction and cumulative partition fraction for store i both approach the same value (Appendix A4, Eq. A29):

$$\frac{x'_i(t)}{f_1(t)} = \frac{x_i(t)}{Q_1(-\infty, t)} = \sum_m \frac{a_{i1}^{(m)}}{r_1 + \lambda^{(m)}} + \text{transient} \quad (8)$$

where $Q_1(-\infty, t)$ is the cumulative forcing in the first component of \mathbf{x} . This is a weighted sum of the constant partition ratios $r_1/(r_1 + \lambda^{(m)})$ for different modes m (compare with Eq. 7). The approach to this value occurs at a rate greater than r_1 , for stable systems with $\lambda^{(m)} > 0$.

The key implication of the above theory is that for a LinExp system, all ratios among fluxes and perturbation state variables approach constant values. This occurs because

Exponential eigenmodes of the carbon-climate system

M. R. Raupach

Title Page

Abstract

Introduction

Conclusions

References

Tables

Figures

⏪

⏩

◀

▶

Back

Close

Full Screen / Esc

Printer-friendly Version

Interactive Discussion



all linear systems of the class of Eq. (2) have exponential eigenfunctions, so that an exponential forcing function yields a response in which all state variables and response fluxes grow exponentially with the same growth rate as the forcing. Moreover, the system response locks onto constancy of ratios among fluxes and state variables at a rate determined by the forcing flux (r_1 in Eq. 8), not the turnover rates for individual state variables (the elements of the system response matrix \mathbf{K}) or normal modes (the eigenvalues $\lambda^{(m)}$ of \mathbf{K}). This means that even for state variables with very slow turnover rates, constant partition fractions and cumulative partition fractions are reached relatively quickly when the forcing grows rapidly (Bacastow and Keeling, 1979).

3 Comparing linear theory with observations

When the carbon-climate system is idealised as a LinExp system, constancy of ratios among fluxes and perturbation state variables implies that the following ratios are all constant: the CO_2 airborne fraction, the cumulative airborne fraction, other CO_2 partition and cumulative partition fractions into land and ocean stores, CO_2 sink rates, and the ratio (T/Q_E) of warming (T) to cumulative CO_2 emissions (Q_E). These predictions can all be tested.

3.1 CO_2 airborne fraction, cumulative airborne fraction and sink rate

The atmospheric CO_2 mass balance is (Le Quéré et al., 2009):

$$c'_A = f_E + f_L + f_M \quad (9)$$

where c_A is the perturbation atmospheric CO_2 store in PgC ($2.127([\text{CO}_2] - [\text{CO}_2]_q)$, with $[\text{CO}_2]$ the CO_2 mixing ratio in ppm and $[\text{CO}_2]_q = 280 \text{ ppm} = [\text{CO}_2]$ at preindustrial equilibrium); $c'_A = dc_A/dt$ is the atmospheric CO_2 accumulation rate; f_E is the total CO_2 emission flux ($f_E = f_{\text{Fossil}} + f_{\text{LUC}}$, including emissions from fossil fuels and other industry, f_{Fossil} , and from net land use change, f_{LUC}); and f_L and f_M are the CO_2 land (L) and

ocean (M, marine) exchange fluxes. All fluxes are positive into the atmosphere. The cumulative CO₂ mass balance is the integral of Eq. (9) from 1750 (a nominal preindustrial time) to t , denoting cumulative fluxes as Q and taking $c_A = 0$ at 1750:

$$c_A = Q_E + Q_L + Q_M, \quad Q_E(t) = \int_{1750}^t f_E(\tau) d\tau. \quad (10)$$

5 Fundamental carbon-cycle partition fractions are the airborne, land and ocean fractions (AF, LF and OF), respectively the fractions of the total CO₂ emission flux remaining in the atmosphere and taken up by natural land and ocean CO₂ sinks:

$$AF = \frac{c'_A}{f_E}, \quad LF = \frac{f'_L}{f_E}, \quad OF = \frac{f'_M}{f_E}. \quad (11)$$

10 Correspondingly, the cumulative airborne, land and ocean fractions (CAF, CLF and COF) are the fractions of cumulative CO₂ emissions (Q_E) appearing in atmospheric, land and ocean stores:

$$CAF = \frac{c_A}{Q_E}, \quad CLF = \frac{Q_L}{Q_E}, \quad COF = \frac{Q_M}{Q_E}. \quad (12)$$

Conservation of mass ensures that $AF + LF + OF = 1$ and $CAF + CLF + COF = 1$.

15 If the carbon cycle obeys the LinExp idealisation, then the partition fractions and cumulative partition fractions are all constant in time and equal for each store, as shown by Eq. (8):

$$\begin{aligned} AF &= CAF = \text{constant} \\ LF &= CLF = \text{constant} \\ OF &= COF = \text{constant.} \end{aligned} \quad (13)$$

Exponential eigenmodes of the carbon-climate system

M. R. Raupach

Title Page	
Abstract	Introduction
Conclusions	References
Tables	Figures
⏪	⏩
◀	▶
Back	Close
Full Screen / Esc	
Printer-friendly Version	
Interactive Discussion	



An observable quantity related to the AF is the CO₂ sink rate k_S , the strength of the combined land and ocean CO₂ sink per unit excess CO₂, with dimension 1/time:

$$k_S = \frac{-f_L - f_M}{c_A} = \frac{f_E - c_A'}{c_A}. \quad (14)$$

The latter equality follows from Eq. (9). The AF and k_S are related diagnostic quantities, because $k_S = (1 - AF) f_E / c_A$, and both can be inferred from observations of f_E and c_A .

The sink rate k_S has several properties: first, it is a measure of the “efficiency” of land and ocean CO₂ sinks, in the sense of sink strength per unit excess CO₂ (Gloor et al., 2010). Second, k_S can be readily split into separate contributions from land and ocean sinks, $k_S = k_L + k_M$, with $k_L = -f_L / c_A$ and $k_M = -f_M / c_A$, to yield separate efficiency measures for land and ocean sinks. Third, $1/k_S$ is a natural time scale for land and ocean CO₂ sinks: it is the e-folding time for the (initially) exponential decay of excess CO₂ that would if emissions were suddenly switched off. Fourth, it can be shown (Appendix A5) that k_S is a weighted sum of rates for CO₂ transfer out of the atmosphere into land and ocean stores with weighting factors dependent on the perturbation carbon stores.

For a LinExp carbon cycle, k_S , k_L and k_M are all constant, because f_L , f_M and c_A all increase exponentially at the same rate (the exponential forcing rate). However, k_S is far from constant with non-exponential emissions, as shown in the next section.

To compare the LinExp predictions for the AF, CAF and k_S with observations, it is first necessary to test whether CO₂ emissions have grown exponentially. Figure 1 (upper panel) compares total CO₂ emissions $f_E(t)$ with an exponential trajectory from 1850 to 2011, using an average growth rate of $1.89\% \text{ yr}^{-1} = (1/53) \text{ yr}^{-1}$ (doubling time 36.7 yr). The short-term growth rate has oscillated around this average value, decreasing below it in the 1980s and 1990s and accelerating above it in the first decade of the 2000s (Le Quéré et al., 2009). Total cumulative CO₂ emissions $Q_E(t)$ have followed an exponential trajectory with the same growth rate remarkably closely since 1850 (Fig. 1, lower panel), apart from a small dip in the two decades before 1950 and a subsequent

Exponential modes of the carbon-climate system

M. R. Raupach

Title Page

Abstract

Introduction

Conclusions

References

Tables

Figures

⏪

⏩

◀

▶

Back

Close

Full Screen / Esc

Printer-friendly Version

Interactive Discussion



recovery in the two following decades. This indicates that departures of emissions $f_E(t)$ from exponential behaviour have not been systematic.

Figure 2 shows the observed AF and CAF (from annual CO₂ data) for 1850 to 2011, suggesting at first sight that the LinExp prediction (AF = CAF = constant) is quite a good approximation. From 1959 to 2011 the average AF was 0.44 ± 0.15 and the average CAF was 0.414 ± 0.011 (1σ over annual values). Observational uncertainties are too large to infer the behaviour of the AF or CAF prior to 1959, the start of the era of in-situ atmospheric CO₂ measurements.

Although the LinExp idealisation is consistent with the observed near constancy of the AF and CAF, further evidence suggests that departures from LinExp behaviour are observable in the carbon cycle. This evidence is of three kinds. First, recent papers (Canadell et al., 2007; Raupach et al., 2008; Le Quéré et al., 2009) have suggested that there is a detectable increasing trend in the AF from 1959 to the early 2000s, at a relative growth rate of 0.2 to 0.3% yr⁻¹. This finding has been contested on several grounds, mainly questioning the attribution of the observed trend in the AF rather than its existence: the observed trend has been attributed to slower-than-exponential growth in f_E (Gloor et al., 2010), to particular events such as volcanic eruptions and ENSO (El Niño-Southern Oscillation) events (Frölicher et al., 2012; Sarmiento et al., 2010), or to errors in CO₂ emissions data in the 1990s and early 2000s (Francey et al., 2010). Reconciliation of these different views on the attribution of observed AF trends is undertaken elsewhere.

Second, the LinExp prediction of constant k_S is tested in Fig. 3 by plotting direct observations of k_S from 1850 to 2011. From 1959 to 2011, k_S declined significantly, by a factor of around 1/3. As with the AF, observational uncertainties prevent statements about trends before 1959. The observed behaviour of k_S is not in accord with the LinExp idealisation, or with the assumption (Gloor et al., 2010) that k_S is constant.

Third, the prediction of a constant CAF is tested in Fig. 4 by plotting the atmospheric CO₂ perturbation (c_A) as a function of cumulative total CO₂ emissions (Q_E). Under the LinExp idealisation this plot would be a straight line, with slope (c_A/Q_E) equal to the

Exponential eigenmodes of the carbon-climate system

M. R. Raupach

Title Page

Abstract

Introduction

Conclusions

References

Tables

Figures



Back

Close

Full Screen / Esc

Printer-friendly Version

Interactive Discussion

CAF. The plot is close to a straight line, but the slope over the recent period (1959 to end of 2011) is higher than over the whole record (1750 to end of 2011), as shown in Table 1. It is not straightforward to assign a statistical significance to the difference between the slopes because the CAF is a highly autocorrelated time series.

5 3.2 Ratio of warming to cumulative emissions

Several recent papers (Allen et al., 2009; Meinshausen et al., 2009; Matthews et al., 2009; Zickfeld et al., 2009) used numerical carbon-climate models proposed a linear or near-linear relationship between global temperature perturbation (T) and cumulative total CO₂ emissions (Q_E):

$$10 \quad T = \alpha Q_E \quad (15)$$

where the slope α is a form of transient climate sensitivity with units KEgC⁻¹ (1 EgC or 1 exagram of carbon is 10¹⁸ gC or 1 trillion tonnes of carbon). From Eq. (8), such a linear relationship holds under a LinExp idealisation of the coupled carbon-climate system, noting that this involves linearised descriptions of processes such as the dependence of radiative forcing on CO₂ and other greenhouse gas concentrations (see Appendix B). The LinExp idealisation identifies conditions under which a proportional relationship between T and Q_E can be expected, and also suggests that proportionality is likely to fail when either or both of the Lin and Exp assumptions break down significantly.

Equation (15) is tested in Fig. 5 by plotting observed T against Q_E . The plot is noisier than Fig. 4 (observed c_A against Q_E) but suggests that Eq. (15) is a useful approximation. As in Fig. 4, the slope over the recent period (1959 to end of 2011; $\alpha = 2.13 \text{ KEgC}^{-1}$) is higher than over the whole record (1750 to 2011; $\alpha = 1.47 \text{ KEgC}^{-1}$) (see Table 2). These values bracket the widely quoted slope in Eq. (15) of $\alpha = 2 \text{ KEgC}^{-1}$ (Allen et al., 2009).

Exponential eigenmodes of the carbon-climate system

M. R. Raupach

Title Page

Abstract

Introduction

Conclusions

References

Tables

Figures

⏪

⏩

◀

▶

Back

Close

Full Screen / Esc

Printer-friendly Version

Interactive Discussion

4 Future breakdown of the LinExp idealisation

Figures 2 to 5 show that the LinExp idealisation applies approximately to the carbon-climate system from 1750 to the present, providing an explanation for the observed near-constancy of the AF, CAF and T/Q_E . It is highly likely that the Lin Exp idealisation will break down in future, causing the AF, CAF and the CO_2 sink rate k_S to depart significantly from constancy. This can happen for one or more of three reasons: departures from linearity (failure of Lin), departures of emissions from exponential trajectories (failure of Exp), and the effects of radiative forcing agents other than CO_2 . Here, these effects are assessed by comparing predictions from the LinExp idealisation with those from a nonlinear model of the carbon-climate system.

4.1 Nonlinear model

The nonlinear model is the Simple-Carbon-Climate Model (SCCM) (Raupach et al., 2011; Harman et al., 2011). The form used here is briefly described Appendix B. SCCM is a globally aggregated model of the carbon-climate system, an approach with long antecedents (for example, Oeschger et al., 1975; also other references for response-function models given in the Introduction). Model state variables are carbon masses in the atmosphere, fast and slow land C stores and a set of ocean C stores; the atmospheric concentrations of CH_4 , N_2O and CFCs; and global perturbation temperature components. Radiative forcing of climate occurs from CO_2 , CH_4 , N_2O , CFCs and aerosols. The model includes nonlinearities of several kinds: the response of terrestrial carbon assimilation to CO_2 , ocean carbonate chemistry, temperature responses of land-air and ocean-air CO_2 exchanges, and the response of radiative forcing to gas concentrations. Model forcing is with prescribed emissions trajectories for CO_2 and non- CO_2 gases. The model also includes the response of terrestrial net primary production to volcanic eruptions, forced with an externally prescribed volcanic aerosol index. SCCM can be linearised analytically, by determining the model Jacobian and thence forming a tangent linear model. The eigenvalues $\lambda^{(m)}$ of \mathbf{K} (the negative of the

Exponential eigenmodes of the carbon-climate system

M. R. Raupach

Title Page

Abstract

Introduction

Conclusions

References

Tables

Figures

⏪

⏩

◀

▶

Back

Close

Full Screen / Esc

Printer-friendly Version

Interactive Discussion



model Jacobian, from Eq. A2) are indeed all positive, confirming that the model is dynamically stable.

To characterise model performance, Fig. 6 shows SCCM predictions for CO₂ concentration [CO₂] and temperature T , with forcing from observed past emissions and analytic scenarios for future emissions of CO₂, CH₄, N₂O and CFCs. Future total CO₂ emissions $f_E(t)$ (top row of Fig. 6) are prescribed using a smooth analytic peak-and-decline trajectory (Raupach et al., 2011) such that the all-time cumulative total CO₂ emission $Q_E(\infty)$ takes values from 1000 to 3000 PgC in 500 PgC steps, with 1000 PgC representing a low-emission, strong mitigation scenario akin to the Representative Concentration Pathway (RCP) scenario RCP3pd, and 3000 PgC a high-emission scenario akin to RCP8.5 (Moss et al., 2010; van Vuuren et al., 2011). Emission trajectories for other gases are the same across all cases (see Appendix B for details). The left panels in Fig. 6 show plots of $f_E(t)$, [CO₂](t) and $T(t)$ against time t , while the right panels show the same quantities plotted against a different clock, cumulative CO₂ emissions $Q_E(t)$ defined by Eq. (10), to yield trajectories $f_E(Q_E)$, [CO₂](Q_E) and $T(Q_E)$.

Figure 6 shows good agreement between SCCM predictions and past observations of [CO₂] and T . For the future, predictions for [CO₂] as a function of Q_E (Fig. 6, middle right panel) are close to straight lines up to near the time of the peak in CO₂, and decline thereafter. (A linear relationship [CO₂](Q_E) is equivalent to a constant CAF = c_A/Q_E). Predictions for T as a function of Q_E (Fig. 6, lower right panel) fall close to a straight line, and agree well with model-ensemble projections from the Fourth Assessment of the Intergovernmental Panel on Climate Change (IPCC AR4) (IPCC, 2007). The slope T/Q_E of this line (about 1.8 K EgC⁻¹) is broadly consistent with the observed past behaviour for this relationship (Fig. 5) and also with the hypothesis of Eq. (15). The different behaviours of [CO₂](Q_E) and $T(Q_E)$ beyond the time of peak CO₂ arise because temperature T declines from its peak much more slowly than CO₂ (Raupach et al., 2011).

Figure 7 shows SCCM predictions of AF, CAF and the CO₂ sink rate k_S , with the same forcing as for Fig. 6. The model reproduces observed past behaviour for all three

Exponential eigenmodes of the carbon-climate system

M. R. Raupach

Title Page

Abstract

Introduction

Conclusions

References

Tables

Figures

⏪

⏩

◀

▶

Back

Close

Full Screen / Esc

Printer-friendly Version

Interactive Discussion

Exponential eigenmodes of the carbon-climate system

M. R. Raupach

Title Page

Abstract

Introduction

Conclusions

References

Tables

Figures

⏪

⏩

◀

▶

Back

Close

Full Screen / Esc

Printer-friendly Version

Interactive Discussion

quantities, apart from interannual variability that is not in the model and is known to be correlated with ENSO (Keeling and Revelle, 1985; Raupach et al., 2008). In the future, the predicted AF varies strongly with CO₂ emissions, decreasing progressively more rapidly as $Q_E(\infty)$ decreases, and becoming negative when the CO₂ concentration starts to decline (Fig. 6, middle row). The CAF is much more conservative but still responds to variation of $Q_E(\infty)$, increasing slightly in future for the high-emission scenario ($Q_E(\infty) = 3000$ PgC) and decreasing for the lowest-emission scenario (1000 PgC), with the decrease occurring mainly beyond the time of peak CO₂, consistent with Fig. 6 (middle right panel). The sink rate k_S declines strongly in all future predictions, by a factor of order 3 from 2000 to 2100 and with further decreases thereafter, continuing a trend already evident in past observations (Fig. 3).

4.2 Attribution of future departures from LinExp

Under the LinExp idealisation, AF, CAF, k_S and T/Q_E would all be constant, with $AF = CAF$ (Eq. 13). For future trajectories of AF, CAF and k_S this is clearly far from the case (Fig. 7), while for T/Q_E , approximate constancy is observed (Fig. 6, lower right panel). To diagnose the reasons for these quite different behaviours, Fig. 8 shows predictions for CO₂ concentration and global temperature (T) from five versions of SCCM at a sequence of levels of simplification ranging from the full nonlinear model to the LinExp idealisation. The same forcing (the high-emission case $Q_E(\infty) = 3000$ PgC in Fig. 6) is used in every version except the last. Schematically, the components in the five model versions are:

- V1 (full model): LinExp + NonExp + NonLin + Coupling + NonCO₂
- V2 (CO₂ only): LinExp + NonExp + NonLin + Coupling
- V3 (uncoupled): LinExp + NonExp + NonLin
- V4 (Lin): LinExp + NonExp
- V5 (LinExp): LinExp

Version 1 (full model) includes all processes represented in SCCM. V2 (CO₂ only) removes radiative forcing from non-CO₂ gases and aerosols. V3 (uncoupled) also removes carbon-climate coupling arising from the dependence of CO₂ fluxes on global temperature (a surrogate for all dependencies of fluxes on physical climate). V4 (Lin) is a fully linearised counterpart of V3 in which all equations for CO₂ fluxes and CO₂ radiative forcing have been linearised, and volcanic influences on the carbon cycle removed. V5 (LinExp) uses the same linearised model as V4, but with an exponential CO₂ emissions trajectory $f_E(t)$.

Considering first the trajectories of [CO₂] and T as functions of time (left panels in Fig. 8), the prediction for [CO₂] shows little response to the removal of non-CO₂ forcing (the step from V1 to V2) except beyond 2100 when warming is large and some decrease in [CO₂] is observed because of carbon-climate coupling. The same simplification step yields a comparable relative decrease in perturbation T (Fig. 8, lower left panel). The removal of nonlinear carbon-climate coupling (step V2 to V3) has a large effect on both [CO₂] and T , decreasing predicted [CO₂] by over 100 ppm (680 to 550) in 2100 with larger decreases thereafter, and decreasing T by a further 0.5 K in 2100 and 1 K in 2200, on top of the decrease from V1 to V2. These responses to carbon-climate coupling are within the range found in carbon-climate model intercomparisons (Friedlingstein et al., 2006; Sitch et al., 2008). The effect of linearisation of CO₂ dynamics and radiative forcing (step V3 to V4) is a moderate additional decrease in [CO₂] and a small additional decrease in T . Finally, imposing an exponential rather than a peak-and-decline CO₂ emissions trajectory (step V4 to V5) has a large effect on both [CO₂] and T , producing exponentially growing perturbation [CO₂] and T in accordance with the above theoretical results for a LinExp system.

The picture is different when trajectories of [CO₂] and T are plotted against cumulative emissions $Q_E(t)$ (right panels in Fig. 8). Using this clock, the full model (V1) produces trajectories [CO₂](Q_E) and $T(Q_E)$ that are close to straight lines. The behaviour of $T(Q_E)$ with the full model replicates Fig. 6 (lower right panel). For [CO₂](Q_E), near-straight-line behaviour is observed up to times a little before the peak in [CO₂],

Exponential eigenmodes of the carbon-climate system

M. R. Raupach

Title Page

Abstract

Introduction

Conclusions

References

Tables

Figures

⏪

⏩

◀

▶

Back

Close

Full Screen / Esc

Printer-friendly Version

Interactive Discussion

Exponential eigenmodes of the carbon-climate system

M. R. Raupach

Title Page

Abstract

Introduction

Conclusions

References

Tables

Figures

⏪

⏩

◀

▶

Back

Close

Full Screen / Esc

Printer-friendly Version

Interactive Discussion



but not thereafter (Raupach et al., 2011) (compare with Fig. 6, middle right panel); this behaviour fills the whole of Fig. 8 (middle right panel) because the peak in CO_2 occurs far in the future under the high-emission scenario used. As the model is simplified sequentially from V1 to V4, the trajectories $[\text{CO}_2](Q_E)$ and $T(Q_E)$ fall progressively below the approximate straight lines for V1, in increments similar to those seen in the corresponding plots against time. The last simplification to reach the LinExp idealisation (V5) yields straight-line trajectories for both $[\text{CO}_2](Q_E)$ and $T(Q_E)$, consistent with theory (Eq. 12). These trajectories are close to those predicted by the full model (V1).

In summary, near-linear behaviour for the trajectories $[\text{CO}_2](Q_E)$ and $T(Q_E)$ is observed at both ends of the model simplification sequence, the full model (V1) and the LinExp idealisation (V5). However, the reasons are quite different in each case. In the LinExp idealisation, linear behaviour is a theoretical requirement following from the fact that a linear system has exponential eigenmodes, so that all ratios among state variables and fluxes are constant when forcing is exponential. For the full model, near-linear behaviour of $[\text{CO}_2](Q_E)$ and $T(Q_E)$ arises from the effects of non- CO_2 radiative forcing, positive feedbacks from carbon-climate coupling, and nonlinear responses of CO_2 fluxes to increasing $[\text{CO}_2]$. Without these effects, $[\text{CO}_2](Q_E)$ and $T(Q_E)$ would both be nonlinear under realistic, non-exponential peak-and-decline emissions trajectories, curving downwards below straight-line behaviour as in model V4 (Fig. 8, right panels). When these effects are included (model V1), the resulting increases in $[\text{CO}_2](Q_E)$ and $T(Q_E)$ restore approximate straight-line behaviour.

Figure 9 shows the effect of model simplification on the AF, CAF and the CO_2 sink rate k_S . In the simplification sequence from V1 to V4, the largest effect occurs with the removal of nonlinear carbon-climate coupling (V2 to V3), causing the AF to decrease strongly and changing both the level and trend in the CAF and k_S . When the LinExp idealisation is reached (V5), constant values for all three quantities are obtained in accordance with theory.

5 Conclusions

The LinExp idealisation provides useful guidance about the past behaviour of the carbon-climate system under strong anthropogenic forcing from 1750 to present, explaining the observed near-constancy of the airborne fraction (AF), the cumulative airborne fraction (CAF) and the ratio T/Q_E of warming to cumulative CO₂ emissions. This idealisation is relevant for the past because three conditions have been approximately satisfied: (1) total CO₂ emissions have increased nearly exponentially (Fig. 1); (2) linearity of carbon cycle response fluxes has been a reasonable approximation (implying that land and ocean sink fluxes have been approximately proportional to excess CO₂ concentration); and (3) there has been approximate cancellation in recent times of the two major classes of radiative forcing other than CO₂, the positive forcing from long-lived non-CO₂ gases (CH₄, N₂O and synthetic gases), and the negative forcing from other agents (mainly aerosols, ozone and albedo effects) (IPCC, 2007, Fig. 2.4).

Nevertheless, departures from the LinExp predictions of constant AF, CAF, CO₂ sink rate (k_S) and T/Q_E are already evident in past observations, particularly in the observed decrease of k_S . These departures will increase as all three of the above conditions break down progressively: (1) emissions will depart from present near-exponential growth (Peters et al., 2011) if mitigation efforts cause trajectories to peak and decline; (2) linearity of carbon cycle responses is likely to be disrupted by increasing nonlinearities as perturbations become larger; (3) the approximate cancellation of non-CO₂ contributions to radiative forcing is unlikely to continue, because of declining negative forcing from non-gaseous agents and increased forcing from non-CO₂ gases (Strassmann et al., 2009; Meinshausen et al., 2011; IIASA, 2012).

The predicted net effect of these factors is that the AF and k_S will depart strongly from constancy in ways that depend on emissions scenarios (Fig. 7): for example, the AF will become negative late in the 21st century under strong mitigation scenarios. However, the predicted ratio T/Q_E continues to be approximately constant in typical scenarios (Fig. 6). This is not because of continued applicability of the LinExp idealisation, but

Exponential eigenmodes of the carbon-climate system

M. R. Raupach

Title Page

Abstract

Introduction

Conclusions

References

Tables

Figures

⏪

⏩

◀

▶

Back

Close

Full Screen / Esc

Printer-friendly Version

Interactive Discussion



instead because of compensating interactions between non-exponential emissions trajectories, nonlinear carbon-cycle dynamics and non-CO₂ gases.

One class of potential nonlinear effects that is of particular concern is the onset of threshold effects not yet evident in the carbon-climate system, typically associated with regional triggers that have global consequences. Examples include large C releases from thawing permafrost soils (Schuur et al., 2008; Tarnocai et al., 2009), major changes in ocean circulation, and loss of the arctic ice sheet through warming. These threshold-like reinforcing feedbacks are not in the model (SCCM) used here, so present conclusions about the future effects of nonlinearities are likely to be conservative.

Appendix A

Mathematical details

A1 Linearised model

Equation (1) is a general representation of a carbon-climate model in which $\mathbf{x}(t)$ is a carbon-climate state vector of matter and energy stores (taken as a perturbation about an equilibrium state $\mathbf{x} = 0$), $\mathbf{f}(t)$ a vector of anthropogenic forcing fluxes, $\Phi(\mathbf{x})$ a vector of system response fluxes, and t time. The state vector \mathbf{x} includes a set of carbon stores in atmospheric, land and ocean reservoirs, a set of physical climate state variables such as land and ocean temperatures and atmospheric water contents. The forcing flux vector $\mathbf{f}(t)$ is externally prescribed. The response flux vector $\Phi(\mathbf{x})$ is the set of net fluxes into the different stores (\mathbf{x}) arising from the response of the system to forcing, and is specified by nonlinear “phenomenological equations” embodying model parameterisations.

The equation system (Eq. 1) can be linearised by approximating $\Phi(\mathbf{x})$ as

$$\Phi(\mathbf{x}) = \Phi_0 - \mathbf{K}(\mathbf{x} - \mathbf{x}_0) \quad (\text{A1})$$

Exponential eigenmodes of the carbon-climate system

M. R. Raupach

Title Page

Abstract

Introduction

Conclusions

References

Tables

Figures

⏪

⏩

◀

▶

Back

Close

Full Screen / Esc

Printer-friendly Version

Interactive Discussion



where $\mathbf{x}_0 = \mathbf{x}(0)$ is the linearisation point (referenced to $t = 0$), $\Phi_0 = \Phi(\mathbf{x}_0)$, and \mathbf{K} is the system response matrix, the negative of the Jacobian matrix of $\Phi(\mathbf{x})$:

$$K_{ij} = - \left[\partial \varphi_i / \partial x_j \right]_{\mathbf{x}=\mathbf{x}_0}. \quad (\text{A2})$$

Diagonal elements of \mathbf{K} are rate constants for flows out of store $i = j$. The linearisation point \mathbf{x}_0 is arbitrary, the simplest option (used in the main text) being to take \mathbf{x}_0 as the initial equilibrium state ($\mathbf{x}_0 = 0$, $\Phi_0 = 0$).

With arbitrary \mathbf{x}_0 , Eq. (1) becomes

$$dx/dt = f(t) + \Phi_0 - \mathbf{K}(\mathbf{x} - \mathbf{x}_0) \quad (\text{A3})$$

with initial condition $\mathbf{x}(0) = \mathbf{x}_0$ and with $\Phi_0 = \Phi(\mathbf{x}_0)$. The solution is:

$$\mathbf{x}(t) = \int_0^t \mathbf{G}(t - \tau) [f(\tau) + \Phi_0 + \mathbf{K}\mathbf{x}_0] d\tau \quad (\text{A4})$$

where the matrix PRF or Green's function is

$$\mathbf{G}(t) = \exp(-\mathbf{K}t) \quad (\text{A5})$$

using the matrix exponential $\exp(\mathbf{M})$, defined for a square matrix \mathbf{M} by

$$\exp(\mathbf{M}) = \sum_{n=0}^{\infty} \frac{\mathbf{M}^n}{n!}. \quad (\text{A6})$$

Equations (A3) and (A4) generalise main-text Eqs. (2) and (3) to arbitrary \mathbf{x}_0 .

Equation (A4) is the multi-dimensional counterpart of the solution for a one-dimensional linear ordinary differential equation (LODE) with constant coefficients:

$$dx/dt = f(t) - kx \quad \text{with} \quad x(0) = x_0. \quad (\text{A7})$$

**Exponential
eigenmodes of the
carbon-climate
system**

M. R. Raupach

Title Page

Abstract

Introduction

Conclusions

References

Tables

Figures

⏪

⏩

◀

▶

Back

Close

Full Screen / Esc

Printer-friendly Version

Interactive Discussion



Here $\mathbf{exp}(\mathbf{K}t)$ reduces to the scalar exponential e^{-kt} , yielding the conventional solution

$$x(t) = \int_0^t e^{-k(t-\tau)} f(\tau) d\tau + e^{-kt} x_0. \quad (\text{A8})$$

A2 Normal modes

5 In the linear system of Eq. (2), let the system response matrix \mathbf{K} have eigenvalues $\lambda^{(m)}$ and eigenvectors $\mathbf{u}^{(m)}$ for modes m , so that

$$\mathbf{K}\mathbf{u}^{(m)} = \mathbf{u}^{(m)} \lambda^{(m)}, \quad \mathbf{K} = \mathbf{U}\mathbf{\Lambda}\mathbf{U}^{-1} \quad (\text{A9})$$

where \mathbf{U} is the matrix of column eigenvectors of \mathbf{K} , and $\mathbf{\Lambda} = \text{diag}(\lambda^{(m)})$ is the diagonal matrix of its eigenvalues. In terms of components $u_i^{(m)}$ of the eigenvectors, components
 10 of \mathbf{U} are $U_{im} = u_i^{(m)}$. The matrices \mathbf{K} , \mathbf{U} and $\mathbf{\Lambda}$ are all square and of the same dimension, and \mathbf{U}^{-1} is a rotation matrix that maps \mathbf{K} to the diagonal matrix $\mathbf{\Lambda}$. This matrix also maps the state vector $\mathbf{x}(t)$ to a new state vector $\mathbf{y}(t)$ of normal modes, such that

$$\mathbf{y} = \mathbf{U}^{-1}\mathbf{x}, \quad \mathbf{x} = \mathbf{U}\mathbf{y}. \quad (\text{A10})$$

Restricting to $x_0 = 0$ (the more general case is similar), Eq. (2) can be rotated to the
 15 new reference frame by premultiplying by \mathbf{U}^{-1} :

$$d\mathbf{y}/dt = \mathbf{U}^{-1}\mathbf{f}(t) - \mathbf{\Lambda}\mathbf{y} \quad \text{with} \quad \mathbf{y}(0) = 0. \quad (\text{A11})$$

For the diagonal matrix $\mathbf{\Lambda}$, $\mathbf{exp}(\mathbf{\Lambda}) = \text{diag}(\exp \lambda^{(m)})$, so Eq. (A11) is a set of independent scalar equations like (Eq. A7) that can be solved one by one. The solution for $\mathbf{y}(t)$ is

$$\mathbf{y}(t) = \int_0^t \mathbf{exp}(-\mathbf{\Lambda}(t-\tau)) \mathbf{U}^{-1} \mathbf{f}(\tau) d\tau. \quad (\text{A12})$$

Exponential eigenmodes of the carbon-climate system

M. R. Raupach

Title Page

Abstract

Introduction

Conclusions

References

Tables

Figures

⏪

⏩

◀

▶

Back

Close

Full Screen / Esc

Printer-friendly Version

Interactive Discussion



Using Eq. (A10), the corresponding solution for $\mathbf{x}(t)$ is:

$$\mathbf{x}(t) = \int_0^t \mathbf{U} \exp(-\mathbf{\Lambda}(t - \tau)) \mathbf{U}^{-1} \mathbf{f}(\tau) d\tau. \quad (\text{A13})$$

This is consistent with the direct solution, Eqs. (A4) and (A5), because the PRF is

$$\mathbf{G}(t) = \exp(-\mathbf{K}t) = \mathbf{U} \exp(-\mathbf{\Lambda}t) \mathbf{U}^{-1} \quad (\text{A14})$$

5 using Eqs. (A6) and (A9).

Equation (A14) shows that the elements of $\mathbf{G}(t)$ are sums of exponential terms with decay rates for different modes (m) given by the eigenvalues $\lambda^{(m)}$ of \mathbf{K} :

$$G_{ij}(t) = \sum_m a_{ij}^{(m)} \exp(-\lambda^{(m)}t) \quad (\text{A15})$$

with

$$10 \quad a_{ij}^{(m)} = U_{im}(U^{-1})_{mj} \quad (\text{A16})$$

(also see Eq. 5). The weights $a_{ij}^{(m)}$ sum over m to 1 when $i = j$ and to 0 otherwise, because $\mathbf{U}\mathbf{U}^{-1} = \mathbf{I}$, the identity matrix. This ensures that $\mathbf{G}(0) = \mathbf{I}$, as required for a PRF.

Equations (A13) to (A15) yield a solution for $\mathbf{x}(t)$ as a sum of convolution integrals with exponential kernels. It is often more useful to compute $\mathbf{x}(t)$ from solutions of independent LODEs, by letting $z_i^{(m)} = U_{im}y_m$ (no sum), a set of rescaled versions of the
 15 normal modes y_m . The $z_i^{(m)}$ are governed by a set of independent LODEs:

$$\frac{dz_i^{(m)}}{dt} = \sum_j a_{ij}^{(m)} f_j(t) - \lambda^{(m)} z_i^{(m)}. \quad (\text{A17})$$

The rescaled normal modes sum to $x_i(t) = \sum_m z_i^{(m)}$.

**Exponential
eigenmodes of the
carbon-climate
system**

M. R. Raupach

Title Page	
Abstract	Introduction
Conclusions	References
Tables	Figures
⏪	⏩
◀	▶
Back	Close
Full Screen / Esc	
Printer-friendly Version	
Interactive Discussion	



A3 Eigenfunctions

With a linear operator $L(\mathbf{x}(t))$, a general inhomogeneous linear system with forcing $\mathbf{f}(t)$ is

$$L(\mathbf{x}(t)) = \mathbf{f}(t). \quad (\text{A18})$$

5 The eigenvalues α and eigenfunctions $\mathbf{v}(t)$ of this system satisfy

$$L(\mathbf{v}(t)) = \alpha \mathbf{v}(t). \quad (\text{A19})$$

For the first-order linear system (Eq. 2), the operator $L(\mathbf{x}(t))$ is given by Eq. (6).

The eigenfunctions of this first-order linear system are exponentials in time. This is demonstrated first for one-dimensional and then for multi-dimensional cases.

10 *One dimension:* In the scalar case, the linear system is governed by Eq. (A7) and its eigenfunctions satisfy $dv/dt + kv = \alpha v$, or $d(\ln v)/dt = \alpha - k$. This implies that

$$v(t) = c e^{(\alpha-k)t} \quad (\text{A20})$$

where c is an arbitrary constant. Equation (A20) is an eigenfunction of Eq. (A7) with any eigenvalue α and constant c . Since these eigenfunctions are exponential, any exponential forcing produces a proportional exponential response. If the forcing for the scalar system is $f(t) = f_0 e^{rt}$, an exponential with growth rate r , then the eigenfunction selected by this forcing is given by $L(\mathbf{v}(t)) = f(t) = \alpha \mathbf{v}(t)$, or

$$f_0 e^{rt} = \alpha c e^{(\alpha-k)t} \quad (\text{A21})$$

which requires that $r = \alpha - k$ and $f_0 = \alpha c$, so that $c = f_0 / (\alpha - k)$. The resulting eigenfunction is therefore

$$v(t) = \frac{f_0}{\alpha - k} e^{rt}. \quad (\text{A22})$$

Exponential eigenmodes of the carbon-climate system

M. R. Raupach

Title Page

Abstract

Introduction

Conclusions

References

Tables

Figures

⏪

⏩

◀

▶

Back

Close

Full Screen / Esc

Printer-friendly Version

Interactive Discussion



Exponential eigenmodes of the carbon-climate system

M. R. Raupach

Title Page

Abstract

Introduction

Conclusions

References

Tables

Figures

⏪

⏩

◀

▶

Back

Close

Full Screen / Esc

Printer-friendly Version

Interactive Discussion



This can be compared with the full solution of Eq. (A7) with $f(t) = f_0 e^{rt}$:

$$x(t) = \frac{f_0}{r+k} e^{rt} + \left(x_0 - \frac{f_0}{r+k} \right) e^{-kt}. \quad (\text{A23})$$

This solution is the sum of the exponential eigenfunction $v(t)$ given by Eq. (A22), and a decaying transient term (taking $k > 0$) that accounts for any difference between the initial condition $x(0) = x_0$ and the initial eigenfunction $v(0) = f_0/(r+k)$. For any initial condition, the full solution approaches the eigenfunction (Eq. A22). The fact that any exponential function is an eigenfunction means that an exponential forcing produces an exponential response with the same growth rate as the forcing.

Multiple dimensions: The eigenfunctions for a multi-dimensional system are easily identified after rotating the state vector $\mathbf{x}(t)$ and its governing system (Eq. 2) to form normal modes $\mathbf{y}(t)$ governed by Eq. (A11). Because the normal modes are independent, the eigenfunctions for each mode m are given by Eq. (A20) with a response rate (k) equal to the eigenvalue $\lambda^{(m)}$ for that mode. When exponential forcing ($f(t) = f_0 e^{rt}$) is applied to that mode, the response is an exponential eigenfunction in that mode, given by Eq. (A22) with $k = \lambda^{(m)}$.

In multi-dimensional systems, forcing (\mathbf{f}) is applied to components of the state vector (\mathbf{x}) rather than to modes (\mathbf{y}). This forcing is distributed among modes as $\mathbf{U}^{-1} \mathbf{f}$ (Eq. A11). When the forcing is exponential, the result is an exponential response in multiple normal modes. An example is a system forced exponentially in just the first component of the state vector \mathbf{x} , so that:

$$\mathbf{f} = (f_{01} e^{r_1 t}, 0, 0, \dots). \quad (\text{A24})$$

The resulting explicit solution for $\mathbf{x}(t)$ in multiple dimensions is the sum $\mathbf{x}(t) = \sum_m \mathbf{z}_i^{(m)}(t)$ of independent scaled normal-mode solutions, each governed by Eq. (A17) and having

a scalar solution given by Eq. (A23). Summing these solutions, the resulting $x(t)$ is

$$x_i(t) = \sum_m \left(\frac{a_{i1}^{(m)} f_{01}}{r_1 + \lambda^{(m)}} \right) e^{r_1 t} + \text{transient} \quad (\text{A25})$$

$$\text{transient} = \sum_m \left(\sum_j a_{ij}^{(m)} x_j(0) - \frac{a_{i1}^{(m)} f_{01}}{r_1 + \lambda^{(m)}} \right) e^{-\lambda^{(m)} t}.$$

- 5 As in the scalar solution, the first term is an exponentially growing eigenfunction and the second a decaying transient term. The weights $a_{ij}^{(m)}$ are given by Eq. (A15).

A4 Ratios among fluxes and state variables

10 Here it is shown that LinExp systems (first-order linear systems with exponential forcing) have the following properties: (a) all state variables grow at forcing rates, not response rates; (b) all ratios among state variables approach constant values; (c) all partition fractions (ratios of growth rates of state variables to the forcing flux) approach constant values; and (d) all ratios become independent of initial conditions at greater than forcing rates.

15 Property (a) is demonstrated by Eq. (A25). To demonstrate properties (b), (c) and (d), the one-dimensional and multi-dimensional cases are dealt with in turn.

One dimension: For the scalar case, Eq. (A7), the solution is Eq. (A8). This solution is characterised by two ratios: the partition fraction $x'(t)/f(t)$, and the cumulative partition fraction $x(t)/Q(-\infty, t)$. Here $Q(-\infty, t)$ is the cumulative forcing

$$Q(-\infty, t) = \int_{-\infty}^t f_0 e^{r\tau} d\tau = \frac{f_0}{r} e^{rt}. \quad (\text{A26})$$

**Exponential
eigenmodes of the
carbon-climate
system**

M. R. Raupach

Title Page	
Abstract	Introduction
Conclusions	References
Tables	Figures
⏪	⏩
◀	▶
Back	Close
Full Screen / Esc	
Printer-friendly Version	
Interactive Discussion	



From Eq. (A23), the partition fraction and the cumulative partition fraction are respectively

$$\frac{x'(t)}{f(t)} = \frac{r}{r+k} - \left(\frac{kx_0}{f_0} - \frac{k}{r+k} \right) e^{-(r+k)t} \quad (\text{A27})$$

$$\frac{x(t)}{Q(-\infty, t)} = \frac{r}{r+k} + \left(\frac{rx_0}{f_0} - \frac{k}{r+k} \right) e^{-(r+k)t}. \quad (\text{A28})$$

Both ratios approach the constant value $r/(r+k)$ (equal to r/α) with a transient term decaying at the rate $r+k$. When r and k are both positive, the decay rate of the transient term is larger than both the forcing rate (r) and the response rate (k).

Multiple dimensions: In this case the partition fractions for the system are the fractions of the forcing flux appearing instantaneously in the stores $x_j(t)$, and the cumulative partition fractions are the ratios of the stores themselves to cumulative forcing. For a system forced exponentially in just the first component of the state vector x (Eq. A24), the partition fractions are

$$\frac{x'_j(t)}{f_1(t)} = \sum_m \frac{a_{j1}^{(m)} f_{01}}{r_1 + \lambda^{(m)}} + \text{transient} \quad (\text{A29})$$

$$\text{transient} = - \sum_m \left(\frac{\lambda^{(m)}}{f_{01}} \sum_j a_{ij}^{(m)} x_j(0) - \frac{a_{j1}^{(m)\lambda^{(m)}}}{r_1 + \lambda^{(m)}} \right) e^{-(r_1 + \lambda^{(m)})t}.$$

This generalises Eq. (A27). As before, a constant plus a decaying transient term are obtained. The cumulative partition fractions are given by a similar expression with the same constant term, as in Eq. (A28). These equations verify properties (b), (c) and (d) for LinExp systems of any dimension.

**Exponential
modes of the
carbon-climate
system**

M. R. Raupach

Title Page

Abstract

Introduction

Conclusions

References

Tables

Figures

⏪

⏩

◀

▶

Back

Close

Full Screen / Esc

Printer-friendly Version

Interactive Discussion

A5 Sink rate

Here it is shown that the sink rate k_S defined by Eq. (14) is a weighted sum of elements of the system response matrix \mathbf{K} for a linearised carbon cycle model. Let the perturbation carbon state vector be $\mathbf{c}(t)$, with component $c_1(t)$ the atmospheric carbon store and $f_1(t)$ the total anthropogenic CO₂ emission flux into the atmosphere. Using Eq. (14), the atmospheric CO₂ mass balance is

$$\frac{dc_1}{dt} = f_1(t) - \sum_j K_{1j} c_j = f_1(t) - k_S c_1 \quad (\text{A30})$$

where the second term in both expressions is the total CO₂ sink flux to land and ocean sinks. Equating these, it follows that

$$k_S = \sum_j K_{1j} c_j. \quad (\text{A31})$$

This shows that k_S is a weighted sum of the elements of \mathbf{K} representing transfer out of store 1 (the atmosphere) into other stores j , where the weighting factors (c_j/c_1) depend on time in general. Only in the particular case where the forcing $f_1(t)$ is exponential (the LinExp idealisation) do the ratios c_j/c_1 and k_S become constant in time.

Appendix B

Simple Carbon-Climate Model

The Simple-Carbon-Climate Model (SCCM) (Raupach et al., 2011; Harman et al., 2011) is a globally aggregated model of the carbon-climate system, mainly based on well-established formulations.

The model state vector is $(c_A, C_{L1}, C_{L2}, c_{Mi}, c_{MD}, [\text{CH}_4], [\text{N}_2\text{O}], [\text{CFC-11}], [\text{CFC-12}], T_{Mi})$; it includes one atmospheric total carbon store (c_A), two land carbon stores (C_{L1} ,

Exponential eigenmodes of the carbon-climate system

M. R. Raupach

Title Page

Abstract

Introduction

Conclusions

References

Tables

Figures

⏪

⏩

◀

▶

Back

Close

Full Screen / Esc

Printer-friendly Version

Interactive Discussion



Exponential eigenmodes of the carbon-climate system

M. R. Raupach

Title Page

Abstract

Introduction

Conclusions

References

Tables

Figures

⏪

⏩

◀

▶

Back

Close

Full Screen / Esc

Printer-friendly Version

Interactive Discussion

C_{L2}), four perturbation carbon stores in the ocean mixed layer (c_{Mi}), one perturbation carbon store in the deep ocean (c_{MD}), atmospheric concentrations of four non-CO₂ greenhouse gases, and three perturbation global temperatures (T_{Mi}). Total and perturbation state variables are denoted by upper and lower-case letters, respectively, and the equilibrium (preindustrial) state by a subscript q (so \mathbf{X} and \mathbf{X}_q are total and equilibrium state vectors, and $\mathbf{x} = \mathbf{X} - \mathbf{X}_q$ is the perturbation about the equilibrium state). An exception to this convention is temperature, where the absolute temperature is Θ and the perturbation temperature is $T = \Theta - \Theta_q$.

Atmospheric carbon: The mass balance for the atmospheric CO₂ store is:

$$C'_A = f_{\text{Foss}} + f_{\text{LUC}} + f_L + f_M \quad (\text{B1})$$

where the prescribed forcing fluxes are $f_{\text{Foss}}(t)$ (CO₂ emissions from fossil fuels and other industry) and $f_{\text{LUC}}(t)$ (emissions from net land use change). The total emission is $f_E = f_{\text{Foss}} + f_{\text{LUC}}$.

Land carbon: The land carbon stores C_{L1} and C_{L2} are the total carbon stores [PgC] in global fast and slow stores, respectively. The governing mass balance equations are

$$dC_{L1}/dt = a_{L1} f_{\text{NPP}} - k_{L1} C_{L1}$$

$$dC_{L2}/dt = a_{L2} f_{\text{NPP}} - k_{L2} C_{L2} - f_{\text{LUC}} \quad (\text{B2})$$

where f_{NPP} is the global terrestrial net primary production (NPP) of biomass carbon [PgC yr⁻¹], k_{Li} is the respiration rate [yr⁻¹] for store i , and a_{Li} is the fraction of global NPP entering store i , with $a_{L1} + a_{L2} = 1$. The respiration rates k_{Li} depend on the global temperature Θ through a q_{10} parameter (the proportional increase in rate for each 10 K of warming). The land use change flux f_{LUC} is withdrawn from the slow land carbon store C_{L2} .

The terrestrial NPP f_{NPP} is a function of CO₂ concentration, modulated by a factor dependent on the volcanic aerosol index (VAI) (Ammann et al., 2003) to account for

Exponential eigenmodes of the carbon-climate system

M. R. Raupach

Title Page

Abstract

Introduction

Conclusions

References

Tables

Figures

⏪

⏩

◀

▶

Back

Close

Full Screen / Esc

Printer-friendly Version

Interactive Discussion

the enhancement of terrestrial NPP by large volcanic eruptions, mainly through the increase in diffuse solar irradiance (Jones and Cox, 2001). The dependence on $[\text{CO}_2]$ is modelled using a power-hyperbolic function $h(x) = x(x^\rho + x_R^\rho)^{-1/\rho}$ ($x \geq 0$), a function that asymptotically approaches x/x_R as $x \rightarrow 0$ and saturates to 1 as $x \rightarrow \infty$, with the power ρ determining the tightness of the curve between the two asymptotes. This functional form allows both a near-linear response of NPP to increasing CO_2 at low excess CO_2 , and a saturating response at high CO_2 . The model is

$$f_{\text{NPP}} = s_1(C_A) s_2(\text{VAI}) \quad (\text{B3})$$

$$s_1(C_A) = f_{\text{NPP}(q)} \left(1 + \frac{(m_{\text{NPP}} - 1) C_A}{(C_A^\rho + C_{\text{NPP}}^\rho)^{1/\rho}} \right)$$

$$s_2(\text{VAI}) = (1 + 0.5 \text{VAI})$$

with preindustrial NPP $f_{\text{NPP}(q)}$, NPP multiplier (saturated/preindustrial) m_{NPP} , slope parameter C_{NPP} , and power parameter ρ . Equation (B3) supplements several earlier options (Raupach et al., 2011; Harman et al., 2011). The factor $(1 + 0.5 \text{VAI})$ accounts for the enhancement of NPP by volcanic aerosol.

The land-atmosphere exchange flux f_L is the negative terrestrial net ecosystem productivity (NEP):

$$f_L = -f_{\text{NEP}} = -(f_{\text{NPP}} - k_{L1} C_{L1} - k_{L2} C_{L2}). \quad (\text{B4})$$

Ocean carbon: Perturbation carbon in the ocean mixed layer (as dissolved inorganic carbon, DIC) is the sum of several stores with different turnover rates k_{Ci} for carbon exchange with the deep ocean. A deep ocean carbon store tracks the carbon transferred downward out of the ocean mixed layer. Mass balances for these perturbation carbon stores are

$$dc_{Mi}/dt = -a_{Ci} f_M - k_{Ci} c_{Mi} \quad (\text{B5})$$

$$dc_{MD}/dt = \sum_i k_{Ci} c_{Mi} \quad (B6)$$

where a_{Ci} is the fraction of the atmosphere-ocean CO_2 flux entering store i , and $\sum a_{Ci} = 1$ over all i . Equation (B5) is equivalent to a pulse-response-function (PRF) formulation for DIC in the ocean mixed layer (Joos et al., 1996; Raupach et al., 2011). The weights a_{Ci} and rates k_{Ci} are specified by a four-term fit to the PRFs from the both the HILDA and box-diffusion advanced ocean models (which have very similar PRFs), thus capturing the ocean dynamics represented in these models (Joos et al., 1996). The ocean-atmosphere flux f_M is a nonlinear function of Θ and c_{Mi} (as DIC) through phenomenological equations (Harman et al., 2011) that emulate full ocean carbonate chemistry (Lewis and Wallace, 1998).

Temperature: Global temperature ($\Theta = \Theta_q + T$) is taken to be the ocean mixed-layer temperature (Θ_M). The perturbation part T_M of Θ_M is the sum of several components, so that $\Theta = \Theta_q + \sum T_{Mj}$. The components T_{Mj} are governed by:

$$dT_{Mj}/dt = b_{Tj} k_{Tj} \lambda_q RF - k_{Tj} T_{Mj} \quad (B7)$$

where RF is the anthropogenic radiative forcing, λ_q is the equilibrium climate sensitivity, and the weights b_{Tj} and rates k_{Tj} characterise the climate step response function (SRF) $1 - \sum b_{Tj} \exp(-k_{Tj}t)$ (Raupach et al., 2011). A three-term climate step response function and associated λ_q from the HadCM3 model (Li and Jarvis, 2009) are used here.

Radiative forcing: This is the sum of contributions from anthropogenic greenhouse gases (CO_2 , CH_4 , N_2O and halocarbons, represented only by CFC-11 and CFC-12), together with aerosols:

$$RF = RF_{CO_2} + RF_{CH_4} + \dots + RF_{Aero} \quad (B8)$$

Conventional expressions are used for radiative forcing as a function of gas concentration (IPCC, 2001, p. 358), specifically $RF_{CO_2} = 5.35 \ln([CO_2]/[CO_2]_q)$. The (negative)

Exponential eigenmodes of the carbon-climate system

M. R. Raupach

Title Page

Abstract

Introduction

Conclusions

References

Tables

Figures

⏪

⏩

◀

▶

Back

Close

Full Screen / Esc

Printer-friendly Version

Interactive Discussion



aerosol forcing is:

$$RF_{\text{Aero}} = c_{\text{Aero}}(t) f_{\text{Foss}}(t) \quad (\text{B9})$$

$$c_{\text{Aero}}(t) = -0.12 \left(1 - \tanh \left((t - 2000)/100 \right) \right).$$

5 This assumes proportional relationships between aerosol radiative forcing, aerosol concentrations, aerosol emissions (taking the aerosol turnover rate to be rapid) and fossil fuel emissions, for instance though sulphate emissions associated with coal combustion. To account for technological improvements, the proportionality coefficient c_{Aero} has a sigmoidal time dependence. Equation (B8) yields $RF = +1.6 \text{ W m}^{-2}$ in 2005 (IPCC, 2007).

10 *Non-CO₂ greenhouse gases:* For CH₄, N₂O and CFCs, total concentrations [X] are determined by the mass balances

$$\frac{d[X]}{dt} = r_X^{-1} (f_{X(\text{Nat})} + f_{X(\text{Anth})}(t)) - k_X [X] \quad (\text{B10})$$

15 with mass-concentration ratios r_X (with units TgCH₄ ppb⁻¹ and likewise for other gases), fluxes f_X (separating natural and anthropogenic components) and atmospheric decay rates k_X . The decay rates for N₂O and CFCs are constant, while that for CH₄ is a weak function of concentration (Raupach et al., 2011) to account for the decrease in CH₄ decay rate from preindustrial to present times (Prinn, 2004). Natural emission fluxes $f_{X(\text{Nat})}$ are taken as time-independent and set to match preindustrial concentrations in the assumed preindustrial equilibrium state.

20 *Forcing:* The forcing fluxes are CO₂ emissions from fossil fuels and other industrial processes (f_{Foss}), CO₂ emissions from net land use change (f_{LUC}), and anthropogenic emission fluxes of CH₄, N₂O and CFCs. For the past, all forcing fluxes are prescribed from data: f_{Foss} from the Carbon Dioxide Information and Analysis Center (CDIAC, 2012); f_{LUC} from R. A. Houghton (GFRA, 2012); recent preliminary estimates of f_{Foss} and f_{Foss} from GCP (2011); and emissions of $f_{X(\text{Anth})}$ for CH₄, N₂O and CFCs from the

Exponential eigenmodes of the carbon-climate system

M. R. Raupach

Title Page

Abstract

Introduction

Conclusions

References

Tables

Figures

⏪

⏩

◀

▶

Back

Close

Full Screen / Esc

Printer-friendly Version

Interactive Discussion



RCP database (Meinshausen et al., 2011; IIASA, 2012). The volcanic aerosol index (Eq. B3) is from Ammann et al. (2003), assuming no volcanic eruptions since 2000.

For the future, forcing fluxes are prescribed with scenarios such as SRES (Nakicenovic et al., 2000), RCP (Meinshausen et al., 2011; IIASA, 2012) or analytic forms.

In Figs. 6 and 7, future $f_{\text{FOSS}}(t)$ is prescribed with a “smooth capped” analytic emissions trajectory that merges an initial exponential-growth phase (with growth rate r) with a mitigation phase in which emissions ultimately decrease exponentially at a mitigation rate m , set to yield specified all-time cumulative emissions $Q_E(\infty)$ (Raupach et al., 2011). Other future analytic emissions trajectories used in Figs. 6 and 7 are: $f_{\text{LUC}}(t)$ decreases linearly from the latest observed value to zero at $t = 2100$; $f_{\text{CH}_4}(t)$ and $f_{\text{N}_2\text{O}}(t)$ are held constant at latest observed values; and CFC emissions decline exponentially at $3\%^{-1}$ (CFC-11) and $6\%^{-1}$ (CFC-12), consistent with RCP scenarios. No volcanic eruptions are postulated in future scenarios.

Parameters: Model parameters, given in Table 3, were set to produce best available agreement with observations from 1850 to 2011 for $[\text{CO}_2]$, AF, k_S , non- CO_2 gas concentrations ($[\text{CH}_4]$, $[\text{N}_2\text{O}]$, [CFC-11], [CFC-12]), and perturbation temperature T . Formal parameter estimation was not used.

Linearisation: The linearised version of SCCM in Figs. 8 and 9 was constructed by linearising the following nonlinear relationships: (1) the relationship between terrestrial NPP and atmospheric $[\text{CO}_2]$ (Eq. B3); (2) the relationship between ocean mixed-layer DIC and $[\text{CO}_2]$ (Lewis and Wallace, 1998; Harman et al., 2011); and (3) the relationship between radiative forcing and $[\text{CO}_2]$. In each case, the nonlinear relationship was replaced with a linearised version giving the same result at $[\text{CO}_2]$ values of 280 ppm (preindustrial) and 400 ppm.

Changes from earlier versions: Relative to earlier SCCM versions (Raupach et al., 2011; Harman et al., 2011), the version used here includes several changes: (1) a new form for terrestrial NPP (Eq. B3); (2) inclusion of a dependence of terrestrial NPP on volcanic eruptions; (3) emulation of full ocean carbonate chemistry (Lewis and Wallace, 1998; Harman et al., 2011); (4) time dependence of cAero (Eq. B9); (5) improved

Exponential eigenmodes of the carbon-climate system

M. R. Raupach

Title Page

Abstract

Introduction

Conclusions

References

Tables

Figures

⏪

⏩

◀

▶

Back

Close

Full Screen / Esc

Printer-friendly Version

Interactive Discussion

data on past emissions of non-CO₂ gases (IIASA, 2012); and (6) minor adjustments to parameters because of these changes.

Appendix C

Data sources

5 Data in figures are from the following sources.

CO₂ emissions from fossil fuels (f_{FOSS}) are from the Carbon Dioxide Information and Analysis Center (CDIAC, 2012). Net CO₂ emissions from land use change (f_{LUC}) are from R. A. Houghton (GFRA, 2012). Recent preliminary emissions estimates and data collation are by the Global Carbon Project (GCP, 2011).

10 Atmospheric CO₂ concentration data prior to 1959 from the Law Dome ice core (Etheridge et al., 1996); for 1959 to 1980 from averaged in situ measurements at Mauna Loa (Hawaii) and the South Pole (Scripps CO₂ Program, 2012); and for 1980 to 2011 from globally averaged in situ data (NOAA-ESRL, 2012).

15 Temperature data are from the Climatic Research Unit (CRU), University of East Anglia, UK (CRU, 2012), the Goddard Institute for Space Studies, USA (NASA-GISS, 2012), and the National Climatic Data Center, USA (NOAA-NCDC, 2012).

20 *Acknowledgements.* I thank Pep Canadell, Philippe Ciais, Ian Enting, Manuel Gloor, Corinne Le Quéré, Jorge Sarmiento, and especially Ian Harman and Cathy Trudinger, for discussions that have helped to motivate and advance the work described here. This work was supported by the Australian Climate Change Research Program (ACCSP) of the Department of Climate Change and Energy Efficiency, Australian Government. The work is a contribution to ACCSP and the Global Carbon Project (<http://www.globalcarbonproject.org/>).

Exponential eigenmodes of the carbon-climate system

M. R. Raupach

Title Page

Abstract

Introduction

Conclusions

References

Tables

Figures

⏪

⏩

◀

▶

Back

Close

Full Screen / Esc

Printer-friendly Version

Interactive Discussion



References

- Allen, M. R., Frame, D. J., Huntingford, C., Jones, C. D., Lowe, J. A., Meinshausen, M., and Meinshausen, N.: Warming caused by cumulative carbon emissions: towards the trillionth tonne, *Nature*, 458, 1163–1166, 2009.
- 5 Ammann, C. M., Meehl, G. A., Washington, W. M., and Zender, C. S.: A monthly and latitudinally varying volcanic forcing dataset in simulations of 20th century climate, *Geophys. Res. Lett.*, 30, 1657, doi:10.1029/2003GL016875, 2003.
- Bacastow, R. B. and Keeling, C. D.: Models to predict future atmospheric CO₂ concentrations, in: *Workshop on the Global Effects of Carbon Dioxide from Fossil Fuels*, edited by: Elliott, W. P. and Machta, L., United States Department of Energy, Washington, D.C., 72–90, 1979.
- 10 Canadell, J. G., Le Quéré, C., Raupach, M. R., Field, C. B., Buitenhuis, E. T., Ciais, P., Conway, T. J., Gillett, N. P., Houghton, R. A., and Marland, G.: Contributions to accelerating atmospheric CO₂ growth from economic activity, carbon intensity, and efficiency of natural sinks, *P. Natl. Acad. Sci. USA*, 104, 18866–18870, 2007.
- 15 CDIAC: Fossil-fuel CO₂ emissions, http://cdiac.ornl.gov/trends/emis/meth_reg.html, Carbon Dioxide Information and Analysis Center, US Department of Energy, last access: 23-7-2012.
- CRU: Global temperature data, <http://www.cru.uea.ac.uk/cru/data/temperature/>, Climatic Research Unit, University of East Anglia, last access: 13 June 2012.
- Drazin, P. G.: *Nonlinear Systems*, Cambridge University Press, Cambridge, p. 317, 1992.
- 20 Enting, I. G.: Laplace transform analysis of the carbon cycle, *Environ. Model. Softw.*, 22, 1488–1497, 2007.
- Etheridge, D. M., Steele, L. P., Langenfelds, R. L., Francey, R. J., Barnola, J. M., and Morgan, V. I.: Natural and anthropogenic changes in atmospheric CO₂ over the last 1000 years from air in Antarctic ice and firn, *J. Geophys. Res.-Atmos.*, 101, 4115–4128, 1996.
- 25 Francey, R. J., Trudinger, C. M., van der Schoot, M., Krummel, P. B., Steele, L. P., and Langenfelds, R. L.: Differences between trends in atmospheric CO₂ and the reported trends in anthropogenic CO₂ emissions, *Tellus B*, 62, 316–328, 2010.
- Friedlingstein, P., Cox, P., Betts, R., Bopp, L., von Bloh, W., Brovkin, V., Cadule, P., Doney, S., Eby, M., Fung, I., Bala, G., John, J., Jones, C., Joos, F., Kato, T., Kawamiya, M., Knorr, W., Lindsay, K., Matthews, H. D., Raddatz, T., Rayner, P., Reick, C., Roeckner, E., Schnitzler, K. G., Schnur, R., Strassmann, K., Weaver, A. J., Yoshikawa, C., and Zeng, N.: Climate-carbon
- 30

ESDD

3, 1107–1158, 2012

Exponential eigenmodes of the carbon-climate system

M. R. Raupach

Title Page

Abstract

Introduction

Conclusions

References

Tables

Figures

⏪

⏩

◀

▶

Back

Close

Full Screen / Esc

Printer-friendly Version

Interactive Discussion

Exponential eigenmodes of the carbon-climate system

M. R. Raupach

Title Page

Abstract

Introduction

Conclusions

References

Tables

Figures

⏪

⏩

◀

▶

Back

Close

Full Screen / Esc

Printer-friendly Version

Interactive Discussion

cycle feedback analysis: Results from the C4MIP model intercomparison, *J. Climate*, 19, 3337–3353, 2006.

Frölicher, T. L., Joos, F., Raible, C. C., and Sarmiento, J. L.: Atmospheric CO₂ response to volcanic eruptions: the role of ENSO, season, and variability, *Global Biogeochemical Cycles*, submitted, 2012.

GCP: Global carbon budget, <http://www.globalcarbonproject.org/carbonbudget/index.htm>, Global Carbon Project, last access: 15 February 2012.

Gershenfeld, N. A.: *The Nature of Mathematical Modeling*, Cambridge University Press, Cambridge, p. 344, 1999.

GFRA: Global Forest Resources Assessment 2010, <http://www.fao.org/forestry/fra/fra2010/en/>, Food and Agriculture Organization, last access: 11 June 2012.

Glendinning, P.: *Stability, Instability and Chaos: an Introduction to the Theory of Nonlinear Differential Equations*, Cambridge University Press, Cambridge, 1–388, 1994.

Gloor, M., Sarmiento, J. L., and Gruber, N.: What can be learned about carbon cycle climate feedbacks from the CO₂ airborne fraction?, *Atmos. Chem. Phys.*, 10, 7739–7751, doi:10.5194/acp-10-7739-2010, 2010.

Hansen, J. E., Sato, M., Kharecha, P., Beerling, D. J., Masson-Delmotte, V., Pagani, M., Raymo, M., Royer, D., and Zachos, J.: Target Atmospheric CO₂: Where Should Humanity Aim?, *Open Atmos. Sci. J.*, 2, 217–231, 2008.

Harman, I. N., Trudinger, C. M., and Raupach, M. R.: SCCM – the Simple Carbon-Climate Model: technical documentation, CAWCR Technical Report no. 47, Centre for Australian Weather and Climate Research, Bureau of Meteorology and CSIRO, Melbourne, Australia, 2011.

Hasselmann, K., Hasselmann, S., Giering, R., Ocana, V., and VonStorch, H.: Sensitivity study of optimal CO₂ emission paths using a simplified structural integrated assessment model (SIAM), *Climatic Change*, 37, 345–386, 1997.

Hooss, G., Voss, R., Hasselmann, K., Maier-Reimer, E., and Joos, F.: A nonlinear impulse response model of the coupled carbon cycle-climate system (NICCS), *Clim. Dynam.*, 18, 189–202, 2001.

Huntingford, C. and Cox, P. M.: An analogue model to derive additional climate change scenarios from existing GCM simulations, *Clim. Dynam.*, 16, 575–586, 2000.

IIASA: RCP Database, version 2.0, International Institute for Applied Systems Analysis, Laxenburg, Austria, 17 June 2012.

Exponential eigenmodes of the carbon-climate system

M. R. Raupach

Title Page

Abstract

Introduction

Conclusions

References

Tables

Figures

⏪

⏩

◀

▶

Back

Close

Full Screen / Esc

Printer-friendly Version

Interactive Discussion

IPCC: Climate Change 2001: The Scientific Basis, Contribution of Working Group I to the Third Assessment Report of the Intergovernmental Panel on Climate Change, edited by: Houghton, J. T., Ding, Y., Griggs, D. J., Noguer, M., van der Linden, P. J., Dai, X., Maskell, K., and Johnson, C. A., Cambridge University Press, Cambridge, UK and New York, 2001.

IPCC: Climate Change 2007: The Physical Science Basis, Contribution of Working Group I to the Fourth Assessment Report of the Intergovernmental Panel on Climate Change, Cambridge University Press, Cambridge, UK and New York, NY, USA, p. 996, 2007.

Jones, C. D. and Cox, P. M.: Modeling the volcanic signal in the atmospheric CO₂ record, *Global Biogeochem. Cy.*, 15, 453–465, 2001.

Joos, F., Bruno, M., Fink, R., Siegenthaler, U., Stocker, T. F., and Le Quéré, C.: An efficient and accurate representation of complex oceanic and biospheric models of anthropogenic carbon uptake, *Tellus B*, 48, 397–417, 1996.

Joos, F., Prentice, I. C., Sitch, S., Meyer, R., Hooss, G., Plattner, G. K., Gerber, S., and Hasselmann, K.: Global warming feedbacks on terrestrial carbon uptake under the Intergovernmental Panel on Climate Change (IPCC) emission scenarios, *Global Biogeochem. Cy.*, 15, 891–907, 2001.

Joos, F., Roth, R., Fuglestedt, J. S., Peters, G. P., Enting, I. G., von Bloh, W., Brovkin, V., Burke, E. J., Eby, M., Edwards, N. R., Friedrich, T., Frölicher, T. L., Halloran, P. R., Holden, P. B., Jones, C., Kleinen, T., Mackenzie, F., Matsumoto, K., Meinshausen, M., Plattner, G.-K., Reisinger, A., Segschneider, J., Shaffer, G., Steinacher, M., Strassmann, K., Tanaka, K., Timmermann, A., and Weaver, A. J.: Carbon dioxide and climate impulse response functions for the computation of greenhouse gas metrics: a multi-model analysis, *Atmos. Chem. Phys. Discuss.*, 12, 19799–19869, doi:10.5194/acpd-12-19799-2012, 2012.

Keeling, C. D. and Revelle, R.: Effects of El-Nino Southern Oscillation on the Atmospheric Content of Carbon-Dioxide, *Meteoritics*, 20, 437–450, 1985.

Le Quéré, C., Raupach, M. R., Canadell, J. G., Marland, G., Bopp, L., Ciais, P., Conway, T. J., Doney, S. C., Feely, R. A., Foster, P., Friedlingstein, P., Gurney, K. R., Houghton, R. A., House, J. I., Huntingford, C., Levy, P. E., Lomas, M. R., Majkut, J., Metzler, N., Ometto, J., Peters, G. P., Prentice, I. C., Randerson, J. T., Running, S. W., Sarmiento, J. L., Schuster, U., Sitch, S., Takahashi, T., Viovy, N., van der Werf, G. R., and Woodward, F. I.: Trends in the sources and sinks of carbon dioxide, *Nat. Geosci.*, 2, 831–836, doi:10.1038/NGEO689, 2009.

Exponential eigenmodes of the carbon-climate system

M. R. Raupach

Title Page

Abstract

Introduction

Conclusions

References

Tables

Figures

⏪

⏩

◀

▶

Back

Close

Full Screen / Esc

Printer-friendly Version

Interactive Discussion



Lewis, E. and Wallace, D. J. Program developed for CO₂ system calculations, ORNL-CDIAC-105, Carbon Dioxide Information Analysis Center, Oak Ridge National Laboratory, Oak Ridge, Tennessee, 38, 1998.

Li, S. and Jarvis, A.: Long run surface temperature dynamics of an A-OGCM: the HadCM3 4 × CO₂ forcing experiment revisited, *Clim. Dynam.*, 33, 817–825, 2009.

Li, S., Jarvis, A. J., and Leedal, D. T.: Are response function representations of the global carbon cycle ever interpretable?, *Tellus B*, 61, 361–371, 2009.

Matthews, H. D., Gillett, N. P., Stott, P. A., and Zickfeld, K.: The proportionality of global warming to cumulative carbon emissions, *Nature*, 459, 829–833, 2009.

Meinshausen, M., Meinshausen, N., Hare, W., Raper, S. C. B., Frieler, K., Knutti, R., Frame, D. J., and Allen, M. R.: Greenhouse gas emission targets for limiting global warming to 2 degC, *Nature*, 458, 1158–1162, 2009.

Meinshausen, M., Smith, S. J., Calvin, K., Daniel, J. S., Kainuma, M. L. T., Lamarque, J. F., Matsumoto, K., Montzka, S. A., Raper, S. C. B., Riahi, K., Thomson, A., Velders, G. J. M., and van Vuuren, D. P. P.: The RCP greenhouse gas concentrations and their extensions from 1765 to 2300, *Climatic Change*, 109, 213–241, 2011.

Moss, R. H., Edmonds, J. A., Hibbard, K. A., Manning, M. R., Rose, S. K., van Vuuren, D. P., Carter, T. R., Emori, S., Kainuma, M., Kram, T., Meehl, G. A., Mitchell, J. F. B., Nakicenovic, N., Riahi, K., Smith, S. J., Stouffer, R. J., Thomson, A. M., Weyant, J. P., and Wilbanks, T. J.: The next generation of scenarios for climate change research and assessment, *Nature*, 463, 747–756, 2010.

Nakicenovic, N., Alcamo, J., Davis, G., de Vries, B., Fenhann, J., Gaffin, S., Gregory, K., Grubler, A., Jung, T. Y., Kram, T., La Rovere, E. L., Michaelis, L., Mori, S., Morita, T., Pepper, W., Pitcher, H., Price, L., Raihi, K., Roehrl, A., Rogner, H.-H., Sankovski, A., Schlesinger, M., Shukla, P., Smith, S., Swart, R., van Rooijen, S., Victor, N., and Dadi, Z.: IPCC Special Report on Emissions Scenarios, Cambridge University Press, Cambridge, UK and New York, p. 599, 2000.

NASA-GISS: GISS surface temperature analysis (GISTEMP), <http://data.giss.nasa.gov/gistemp/>, National Aeronautics and Space Administration, USA, last access: 13 June 2012.

NOAA-ESRL: Trends in Atmospheric Carbon Dioxide, <http://www.esrl.noaa.gov/gmd/ccgg/trends/>, Earth System Research Laboratory, National Oceanic and Atmospheric Administration, last access: 13 June 2012.

Exponential eigenmodes of the carbon-climate system

M. R. Raupach

Title Page

Abstract

Introduction

Conclusions

References

Tables

Figures

⏪

⏩

◀

▶

Back

Close

Full Screen / Esc

Printer-friendly Version

Interactive Discussion



NOAA-NCDC: Global surface temperature anomalies, <http://www.ncdc.noaa.gov/cmb-faq/anomalies.php>, National Climatic Data Center, National Oceanic and Atmospheric Administration, USA, last access: 13 June 2012.

Oeschger, H., Siegenthaler, U., Schotterer, U., and Gugelmann, A.: Box Diffusion-Model to Study Carbon-Dioxide Exchange in Nature, *Tellus B*, 27, 168–192, 1975.

Peters, G. P., Marland, G., Le Quéré, C., Boden, T. A., Canadell, J. G., and Raupach, M. R.: Rapid growth in CO₂ emissions after the 2008–2009 Global Financial Crisis, *Nat. Clim. Change*, 2, 2–4, 2011.

Petschel-Held, G., Schellnhuber, H. J., Bruckner, T., Toth, F. L., and Hasselmann, K.: The tolerable windows approach: Theoretical and methodological foundations, *Climatic Change*, 41, 303–331, 1999.

Prinn, R. G.: Non-CO₂ greenhouse gases, in: *The Global Carbon Cycle: Integrating Humans, Climate, and the Natural World*, edited by: Field, C. B. and Raupach, M. R., Island Press, Washington, 205–216, 2004.

Raper, S. C. B., Gregory, J. M., and Osborn, T. J.: Use of an upwelling-diffusion energy balance climate model to simulate and diagnose A/OGCM results, *Clim. Dynam.*, 17, 601–613, 2001.

Raupach, M. R., Canadell, J. G., and Le Quéré, C.: Anthropogenic and biophysical contributions to increasing atmospheric CO₂ growth rate and airborne fraction, *Biogeosciences*, 5, 1601–1613, doi:10.5194/bg-5-1601-2008, 2008.

Raupach, M. R., Canadell, J. G., Ciais, P., Friedlingstein, P., Rayner, P. J., and Trudinger, C. M.: The relationship between peak warming and cumulative CO₂ emissions, and its use to quantify vulnerabilities in the carbon-climate-human system, *Tellus B*, 63, 145–164, 2011.

Sarmiento, J. L., Gloor, M., Gruber, N., Beaulieu, C., Jacobson, A. R., Mikaloff Fletcher, S. E., Pacala, S., and Rodgers, K.: Trends and regional distributions of land and ocean carbon sinks, *Biogeosciences*, 7, 2351–2367, doi:10.5194/bg-7-2351-2010, 2010.

Schuur, E. A. G., Bockheim, J., Canadell, J. G., Euskirchen, E., Field, C. B., Goryachkin, S. V., Hagemann, S., Kuhry, P., Laffleur, P., Lee, H., Mazhitova, G., Nelson, F. E., Rinke, A., Romanovsky, V. E., Shiklomanov, N., Tarnocai, C., Venevsky, S., Vogel, J. G., and Zimov, S. A.: Vulnerability of permafrost carbon to climate change: implications for the global carbon cycle, *BioScience*, 58, 701–714, 2008.

Scripps CO₂ Program: Atmospheric CO₂ data, <http://scrippsco2.ucsd.edu/data/data.html>, Scripps Institution of Oceanography, last access: 13 June 2012.

Exponential eigenmodes of the carbon-climate system

M. R. Raupach

Title Page

Abstract

Introduction

Conclusions

References

Tables

Figures

⏪

⏩

◀

▶

Back

Close

Full Screen / Esc

Printer-friendly Version

Interactive Discussion



- Sitch, S., Huntingford, C., Gedney, N., Levy, P. E., Lomas, M., Piao, S. L., Betts, R., Ciais, P., Cox, P., Friedlingstein, P., Jones, C. D., Prentice, I. C., and Woodward, F. I.: Evaluation of the terrestrial carbon cycle, future plant geography and climate-carbon cycle feedbacks using five Dynamic Global Vegetation Models (DGVMs), *Global Change Biol.*, 14, 2015–2039, 2008.
- 5 Strassmann, K. M., Plattner, G. K., and Joos, F.: CO₂ and non-CO₂ radiative forcings in climate projections for twenty-first century mitigation scenarios, *Clim. Dynam.*, 33, 737–749, 2009.
- Tarnocai, C., Canadell, J. G., Schuur, E. A. G., Kuhry, P., Mazhitova, G., and Zimov, S. A.: Soil organic carbon pools in the northern circumpolar permafrost region, *Global Biogeochem. Cy.*, 23, GB2023, doi:10.1029/2008GB003327, 2009.
- 10 Trudinger, C. M., Enting, I. G., Rayner, P. J., and Francey, R. J.: Kalman filter analysis of ice core data – 2. Double deconvolution of CO₂ and delta C¹³ measurements, *J. Geophys. Res.-Atmos.*, 107, 4422, 2002.
- van Vuuren, D. P., Edmonds, J., Kainuma, M., Riahi, K., Thomson, A., Hibbard, K., Hurtt, G. C., Kram, T., Krey, V., Lamarque, J. F., Masui, T., Meinshausen, M., Nakicenovic, N., Smith, S. J., and Rose, S. K.: The representative concentration pathways: an overview, *Climatic Change*, 109, 5–31, 2011.
- 15 Zickfeld, K., Eby, M., Matthews, H. D., and Weaver, A. J.: Setting cumulative emissions targets to reduce the risk of dangerous climate change, *P. Natl. Acad. Sci. USA*, 106, 16129–16134, 2009.

Exponential eigenmodes of the carbon-climate system

M. R. Raupach

Table 1. Linear regression coefficients for atmospheric CO₂ perturbation c_A as a function of cumulative total CO₂ emissions Q_E (Fig. 4). Parameter uncertainties are 1σ standard errors without accounting for autocorrelation.

Period	Fit	Coefficients	r^2
1750–2011.99	$c_A = a_1 Q_E$	$a_1 = 0.421 \pm 0.002$ $a_0 = 0$	0.997
1960–2011.99	$c_A = a_0 + a_1 Q_E$	$a_1 = 0.445 \pm 0.002$ $a_0 = -11.08 \pm 0.82$	0.997

[Title Page](#)
[Abstract](#)
[Introduction](#)
[Conclusions](#)
[References](#)
[Tables](#)
[Figures](#)
[⏪](#)
[⏩](#)
[◀](#)
[▶](#)
[Back](#)
[Close](#)
[Full Screen / Esc](#)
[Printer-friendly Version](#)
[Interactive Discussion](#)


Exponential eigenmodes of the carbon-climate system

M. R. Raupach

Table 2. Linear regression coefficients for global temperature perturbation T as a function of cumulative total CO₂ emissions Q_E (Fig. 5). Parameter uncertainties are 1σ standard errors without accounting for autocorrelation.

Period	Fit	Coefficients	r^2
1750–2011.99	$T_A = a_1 Q_E$	$a_1 = 1.47 \pm 0.05 \text{ KEgC}^{-1}$ $a_0 = 0 \text{ K}$	0.87
1960–2011.99	$T_A = a_0 + a_1 Q_E$	$a_1 = 2.13 \pm 0.13 \text{ KEgC}^{-1}$ $a_0 = -0.23 \pm 0.05 \text{ K}$	0.83

[Title Page](#)
[Abstract](#)
[Introduction](#)
[Conclusions](#)
[References](#)
[Tables](#)
[Figures](#)
[⏪](#)
[⏩](#)
[◀](#)
[▶](#)
[Back](#)
[Close](#)
[Full Screen / Esc](#)
[Printer-friendly Version](#)
[Interactive Discussion](#)

Table 3. Parameters in SCCM. R2011 refers to Raupach et al. (2011).

Parameter	Eqn	Symbol	Units	Value
Equilibrium terrestrial NPP	(B3)	$f_{\text{NPP}(q)}$	PgC yr ⁻¹	40.0
NPP multiplier	(B3)	m_{NPP}	–	1.5
NPP slope parameter	(B3)	c_{NPP}	PgC	687
NPP power parameter	(B3)	p	–	2.5
Equilibrium respiration rate		$k_{\text{L1}(q)}$	yr ⁻¹	1/2.5
Equilibrium respiration rate		$k_{\text{L2}(q)}$	yr ⁻¹	1/250
q_{10} for respiration		q_{10}	–	2.0
NPP partition fraction	(B2)	a_{L1}	–	0.5
NPP partition fraction	(B2)	a_{L2}	–	$1 - a_{\text{L1}}$
Air-ocean gas exchange rate		k_{Gas}	yr ⁻¹	1/8.76
Equilibrium DIC		DIC_q	molC m ⁻³	2.089
Equilibrium temperature		Θ_q	degC	15
Equilibrium [CO ₂]		$[\text{CO}_2]_q$	ppm	280
Equilibrium land C stores		C_{Li}	PgC	$\frac{a_{\text{Li}} f_{\text{NPP}(q)}}{k_{\text{Li}}(q)}$
Ocean CO ₂ PRF: weights	(B5)	a_{Ci}	–	R2011
Ocean CO ₂ PRF: rates	(B5)	k_{Ci}	yr ⁻¹	R2011
Non-CO ₂ gases: decay rates	R2011	k_{X}	yr ⁻¹	R2011
Non-CO ₂ gases: equilibria	R2011	$[\text{X}]_q$	ppb	R2011
Coefficient for aerosol RF	(B9)	c_{Aero}	RF/[f_{FFoss}]	(B9)
Climate SRF: weights	(B7)	b_{Tj}	–	R2011
Climate SRF: rates	(B7)	k_{Tj}	yr ⁻¹	R2011
Equil climate sensitivity	(B7)	λ_q	KW ⁻¹ m ²	R2011

Exponential eigenmodes of the carbon-climate system

M. R. Raupach

Title Page

Abstract

Introduction

Conclusions

References

Tables

Figures

⏪

⏩

◀

▶

Back

Close

Full Screen / Esc

Printer-friendly Version

Interactive Discussion

Exponential eigenmodes of the carbon-climate system

M. R. Raupach

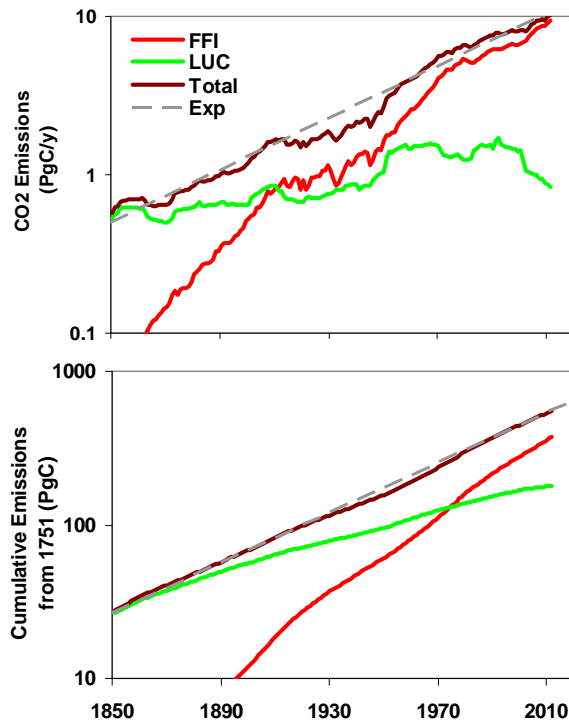


Fig. 1. Upper panel: observed total global CO₂ emissions, $f_E = f_{\text{FOSS}} + f_{\text{LUC}}$, as a function of time. Lower panel: cumulative global CO₂ emissions, $Q_E = Q_{\text{FOSS}} + Q_{\text{LUC}}$. The vertical axis in both panels is logarithmic so that exponentially growing emissions would appear as a straight line. The dashed line in both panels indicates exponential growth, proportional to e^{rt} with $r = 1.89\% \text{ yr}^{-1}$. Data sources: Appendix C.

[Title Page](#)
[Abstract](#)
[Introduction](#)
[Conclusions](#)
[References](#)
[Tables](#)
[Figures](#)
[◀](#)
[▶](#)
[◀](#)
[▶](#)
[Back](#)
[Close](#)
[Full Screen / Esc](#)
[Printer-friendly Version](#)
[Interactive Discussion](#)

Exponential eigenmodes of the carbon-climate system

M. R. Raupach

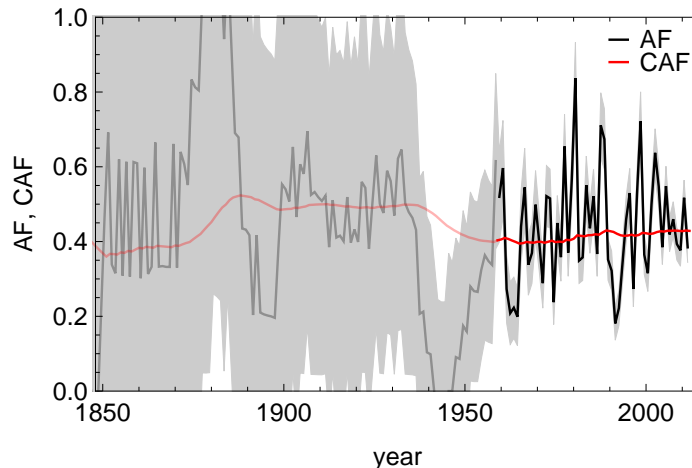


Fig. 2. Observed CO₂ airborne fraction (AF, Eq. 11) and cumulative airborne fraction (CAF, Eq. 12). The grey band is an uncertainty estimate ($\pm 1\sigma$) for $AF = c'_A/f_E$, accounting for errors in both CO₂ emissions ($f_E = f_{\text{Foss}} + f_{\text{LUC}}$) and atmospheric accumulation ($c'_A = dc_A/dt$, calculated from annual increments in c_A). An uncertainty band for CAF is not shown here for clarity (it is shown elsewhere; see Figs. 7 and 9). Full and semi-transparent lines for both AF (black) and CAF (red) respectively denote the observations in the period of high-quality in situ atmospheric CO₂ estimates (from 1959 onward) and the period before 1959 for which atmospheric CO₂ is inferred from ice core data; the uncertainty is much larger before 1959. Data sources: Appendix C.

Title Page

Abstract

Introduction

Conclusions

References

Tables

Figures

◀

▶

◀

▶

Back

Close

Full Screen / Esc

Printer-friendly Version

Interactive Discussion



Exponential eigenmodes of the carbon-climate system

M. R. Raupach

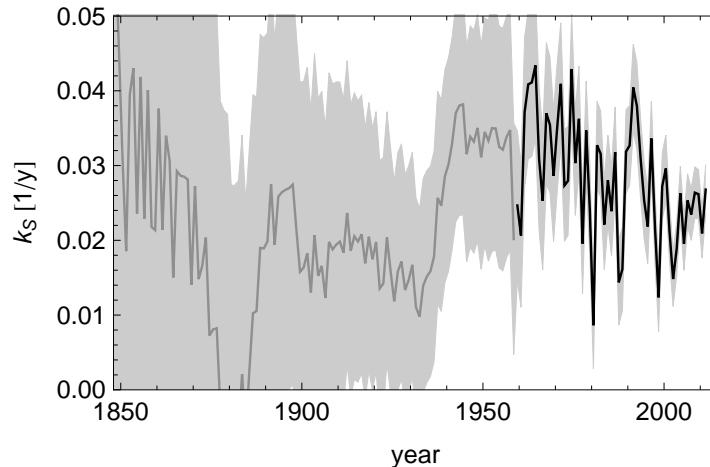


Fig. 3. Observed CO₂ sink rate k_S (Eq. 14). As in Fig. 2, the grey band is an uncertainty estimate ($\pm 1\sigma$) accounting for errors in both CO₂ emissions and CO₂ concentration data, and full and semi-transparent lines respectively denote observations in the period of high-quality in situ atmospheric CO₂ estimates (from 1959 onward) and the period before 1959. Data sources: Appendix C.

[Title Page](#)[Abstract](#)[Introduction](#)[Conclusions](#)[References](#)[Tables](#)[Figures](#)[⏪](#)[⏩](#)[◀](#)[▶](#)[Back](#)[Close](#)[Full Screen / Esc](#)[Printer-friendly Version](#)[Interactive Discussion](#)

Exponential eigenmodes of the carbon-climate system

M. R. Raupach

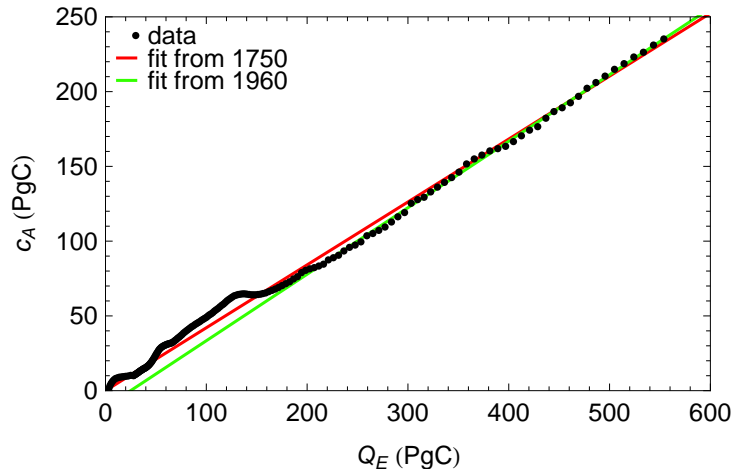


Fig. 4. Perturbation atmospheric CO_2 store (in PgC), $c_A(t)$, as a function of cumulative total CO_2 emissions, $Q_E(t)$. Red line is a linear fit $c_A = a_1 Q_E$ to data from 1750 to end of 2011, constrained to pass through the origin $(Q_E, c_A) = (0, 0)$; the green line is a linear fit $c_A = a_0 + a_1 Q_E$ to data from 1960 to end of 2011, not constrained to pass through the origin. Coefficients a_0 and a_1 are given in Table 1. Data sources: Appendix C.

Title Page

Abstract

Introduction

Conclusions

References

Tables

Figures

◀

▶

◀

▶

Back

Close

Full Screen / Esc

Printer-friendly Version

Interactive Discussion

Exponential eigenmodes of the carbon-climate system

M. R. Raupach

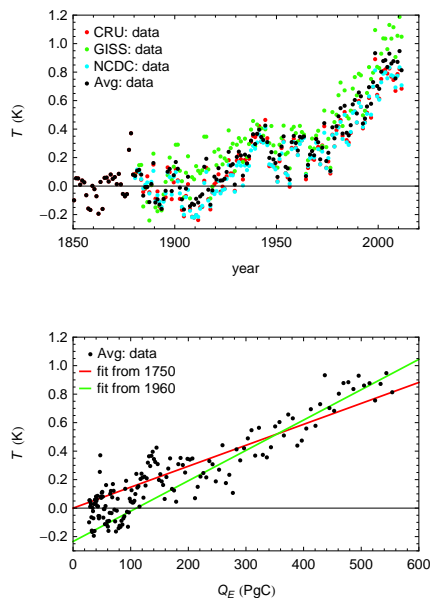


Fig. 5. Perturbation global temperature T (referenced to 1880–1900) from three data sources, as a function of time t (upper panel) and of cumulative CO_2 emissions Q_E (lower panel). The average of all three series is shown as black points. In the lower panel, the red line is a linear fit $T = a_1 Q_E$ to all available T data (average over 3 sources) constrained to pass through the origin $(Q_E, T) = (0, 0)$. The green line is a linear fit $T = a_0 + a_1 Q_E$ to data from 1960 to 2011, not constrained to pass through the origin. Coefficients a_0 and a_1 are given in Table 2. Data sources: Appendix C.

Title Page

Abstract

Introduction

Conclusions

References

Tables

Figures

◀

▶

◀

▶

Back

Close

Full Screen / Esc

Printer-friendly Version

Interactive Discussion

Exponential eigenmodes of the carbon-climate system

M. R. Raupach

Title Page

Abstract

Introduction

Conclusions

References

Tables

Figures

◀

▶

◀

▶

Back

Close

Full Screen / Esc

Printer-friendly Version

Interactive Discussion

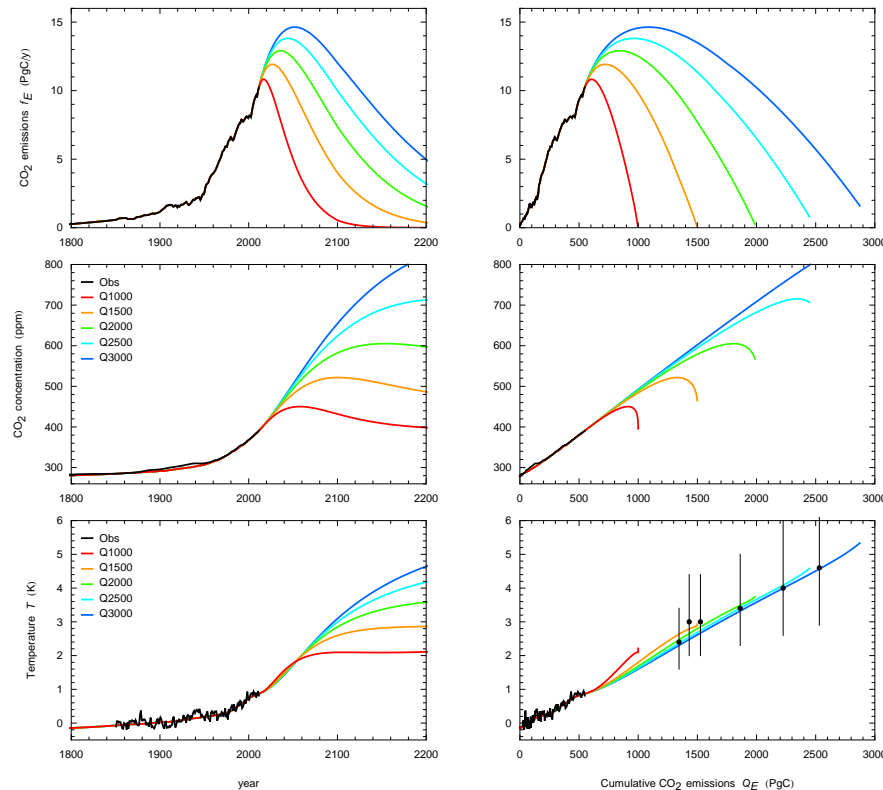


Fig. 6. Total CO_2 emissions (f_E) and predictions for CO_2 concentration and temperature T , with analytic emission scenarios for CO_2 and non- CO_2 gases such that the cumulative total CO_2 emission $Q_E(\infty)$ takes values from 1000 to 3000 PgC. Scenarios are given in Appendix B. Left and right panels show plots against time and $Q_E(t)$, respectively. Points represent IPCC AR4 projections (IPCC, 2007) for $T(Q_E)$ in 2100, for six SRES marker scenarios (from left: B1, A1T, B2, A1B, A2, A1FI), with 17–83% uncertainty ranges. Data sources: Appendix C.

Exponential eigenmodes of the carbon-climate system

M. R. Raupach

Title Page

Abstract

Introduction

Conclusions

References

Tables

Figures

◀

▶

◀

▶

Back

Close

Full Screen / Esc

Printer-friendly Version

Interactive Discussion

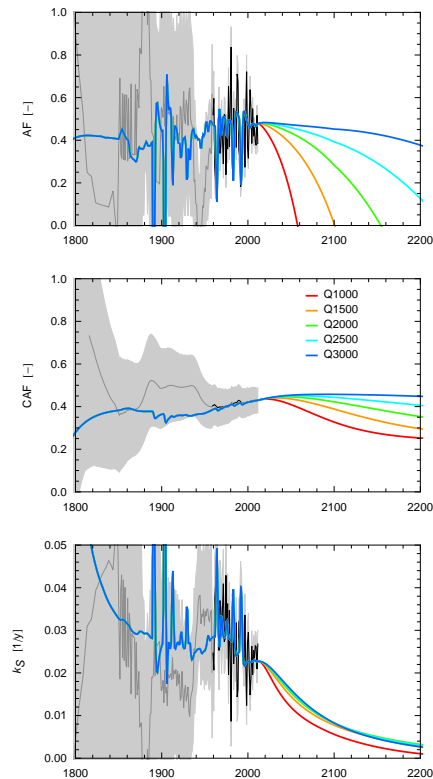


Fig. 7. SCCM predictions of AF, CAF and k_s with analytic scenarios for future emissions of CO₂ and non-CO₂ gases (CH₄, N₂O, CFCs) such that the all-time cumulative total CO₂ emission $Q_E(\infty)$ takes values from 1000 to 3000 PgC. Model details as for Fig. 6. Error bands on observations are $\pm 1\sigma$. Data sources: Appendix C.

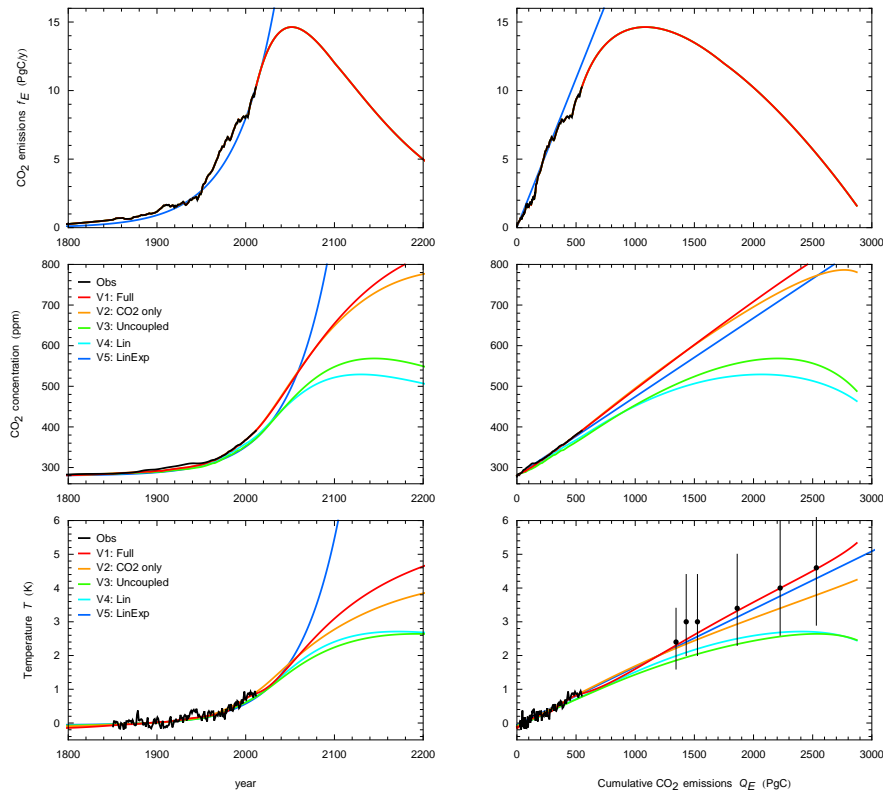


Fig. 8. SCCM predictions of $[\text{CO}_2]$ and T with successive simplification of process descriptions, from a full model to the LinExp idealisation. Model versions: (V1, red) full model; (V2, orange) CO_2 only; (V3, green) uncoupled; (V4, sky blue) Lin; (V5, dark blue) LinExp. Prescribed total CO_2 emissions trajectories are identical for versions V1 to V4, and are exponential for V5. Other details as for Fig. 6. Data sources: Appendix C.

Exponential eigenmodes of the carbon-climate system

M. R. Raupach

Title Page

Abstract Introduction

Conclusions References

Tables Figures

◀ ▶

◀ ▶

Back Close

Full Screen / Esc

Printer-friendly Version

Interactive Discussion



Exponential eigenmodes of the carbon-climate system

M. R. Raupach

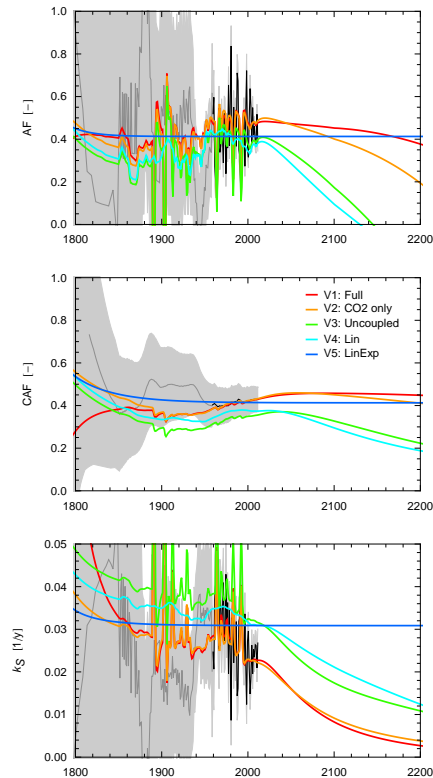


Fig. 9. SCCM predictions of AF, CAF and k_S with successive simplification of process descriptions, from a full model to the LinExp idealisation. Model details as for Fig. 8. Error bands on observations are $\pm 1\sigma$. Data sources: Appendix C.

Title Page

Abstract

Introduction

Conclusions

References

Tables

Figures

◀

▶

◀

▶

Back

Close

Full Screen / Esc

Printer-friendly Version

Interactive Discussion